TU Delft

Delft University of Technology

Uplift of the Transdanubian Range, Pannonian Basin
How fast and why?

RuszkiczayY-Ruediger, Zs; Balázs, A.; Csillag, G.; Drijkoningen, G.; Fodor, L.

DOI
10.1016/j.gloplacha.2020.103263

Publication date
2020

Document Version
Final published version

Published in
Global and Planetary Change

Citation (APA)
RuszkiczayY-Ruediger, Z., Balázs, A., Csillag, G., Drijkoningen, G., & Fodor, L. (2020). Uplift of the Transdanubian Range, Pannonian Basin: How fast and why? *Global and Planetary Change*, *192*, Article 103263. https://doi.org/10.1016/j.gloplacha.2020.103263

Important note
To cite this publication, please use the final published version (if applicable).
Please check the document version above.

Copyright
Other than for strictly personal use, it is not permitted to download, forward or distribute the text or part of it, without the consent of the author(s) and/or copyright holder(s), unless the work is under an open content license such as Creative Commons.

Takedown policy
Please contact us and provide details if you believe this document breaches copyrights.
We will remove access to the work immediately and investigate your claim.

This work is downloaded from Delft University of Technology.
For technical reasons the number of authors shown on this cover page is limited to a maximum of 10.

Global and Planetary Change 192 (2020) 103263

Contents lists available at ScienceDirect

Global and Planetary Change

journal homepage: www.elsevier.com/locate/gloplacha

Uplift of the Transdanubian Range, Pannonian Basin: How fast and why?

Zs Ruszkiczay-Rüdiger[a,*], A. Balázs[b], G. Csillag[a,c], G. Drijkoningen[d], L. Fodor[c,e]

[a] Research Centre for Astronomy and Earth Sciences, Institute for Geological and Geochemical Research, Budaörsi út 45, 1112 Budapest, Hungary
[b] ETH Zurich, Geophysical Fluid Dynamics Group, Institute of Geophysics, Sonneggstrasse 5, 8092 Zurich, Switzerland
[c] MTA-ELTE Geological, Geophysical and Space Science Research Group, Pázmány Péter sétány 1/c, 1117 Budapest, Hungary
[d] Faculty of Civil Engineering and Geosciences, Delft University of Technology, Stevinweg 1, 2628 CN Delft, the Netherlands
[e] ELTE Eötvös University, Department of Physical and Applied Geology, Pázmány Péter sétány 1/c, 1117 Budapest, Hungary

ARTICLE INFO

Keywords:
Terrace chronology
Incision rate
Quaternary
Central Europe
Neotectonics
Lithospheric deformation

ABSTRACT

The cumulative incision rates of ~50–70 m/Ma integrating over the last ~3 Ma have been derived from published terrace-chronological data of the Danube river in the Western Pannonian Basin. An apparent acceleration of uplift rates was observed for shorter timescales culminating at ~200 m/Ma over the last ~140 ka. An examination of the change of the incision rates through time revealed that the incision rate was fairly constant at ~50 m/Ma from ~3 Ma to ~140 ka, and the faster rates are valid only for the last ~140 ka. These findings suggest that the long-term uplift rate of the northwestern limb of the Transdanubian Range is ~50 m/Ma, and the apparent acceleration of river incision during the Late Pleistocene is considered as the result of faster, most probably climate-driven incision during the last glacial cycle, outpacing the long-term uplift rate. The observed upper crustal neotectonic faults are not sufficient to accommodate the deformation necessary for the reported Pliocene to Quaternary vertical motion. The geodynamic model for the explanation of the magnitude and pattern of surface uplift in the western Pannonian Basin involves a complex interplay between (1) deep lithosphere-asthenosphere dynamics, (2) structural inversion governed by the northward drift of Adria, (3) inherited geological structures and (4) climate driven surface processes (denudation and sediment loading).

1. Introduction

Differential vertical movements of rock masses can be induced by variable plate tectonic forces (Burov and Cloetingh, 1997; Viveen et al., 2012; Fuchs et al., 2014) associated to crustal thinning or thickening and its isostatic compensation (Cloetingh et al., 2013). Furthermore, mantle flow-induced vertical stresses and thermal effects control dynamic topography (Lithgow-Bertelloni and Silver, 1998; Demoulin and Hallot, 2009; Horváth et al., 2015; Balázs et al., 2017).

If denudation does not counterbalance the positive vertical motion of rocks, the surface undergoes uplift. In this scenario older landforms and related deposits occupy progressively higher topographic positions. The formation of a terrace system is one expression of such a process (Demoulin et al., 2017). Terrace formation is the result of the sensitive interplay between tectonic and climatic forces (Maddy et al., 2001; Starkel, 2003; Antoine et al., 2007; Finnegan et al., 2014; Olszak, 2017), with terrace aggradation and river incision being influenced by climate oscillations controlling river discharge and sediment load (Vandenberghe, 2015; Bridgland and Westaway, 2008).

Vertically displaced or warped terrace staircases record the amount of deformation relative to a reference level, usually the modern riverbed or the channel thalweg. The age determination of deformed terraces enables the quantification of the rate of river incision (Maddy et al., 2001; Gibbard and Lewin, 2009; Štor et al., 2019). Assuming that the reference level does not change through the deformation, the incision rate is a good approximation of the surface uplift rate. This approach presumes that the incision rates are in equilibrium with external forcing over a wide range of timescales (Finnegan et al., 2014).

The present study aims at the quantification of the Late Pliocene to Quaternary uplift rates in the Pannonian Basin, where two subsiding basins are separated by a hilly ridge, the Transdanubian Range (TR). Our study area at the NW side of the TR represent the transitional zone between the subsiding Danube Basin and uplifting TR, a key position for the understanding of the neotectonic deformation affecting the Pannonian Basin (Fig. 1). A noteworthy feature of the TR is its ca. 600–700 m of Late Miocene to Recent uplift in the absence of high offset thrusts or reverse faults and therefore this pronounced non-isostatic motion coupled with the overall kilometre-scale differential vertical movements affecting the entire Pannonian Basin needs further explanations.

* Corresponding author.
E-mail address: rrzsofi@geochem.hu (Z. Ruszkiczay-Rüdiger).

https://doi.org/10.1016/j.gloplacha.2020.103263
Received 17 March 2020; Received in revised form 11 June 2020; Accepted 12 June 2020
Available online 17 June 2020
0921-8181/ © 2020 The Authors. Published by Elsevier B.V. This is an open access article under the CC BY-NC-ND license (http://creativecommons.org/licenses/BY-NC-ND/4.0/).

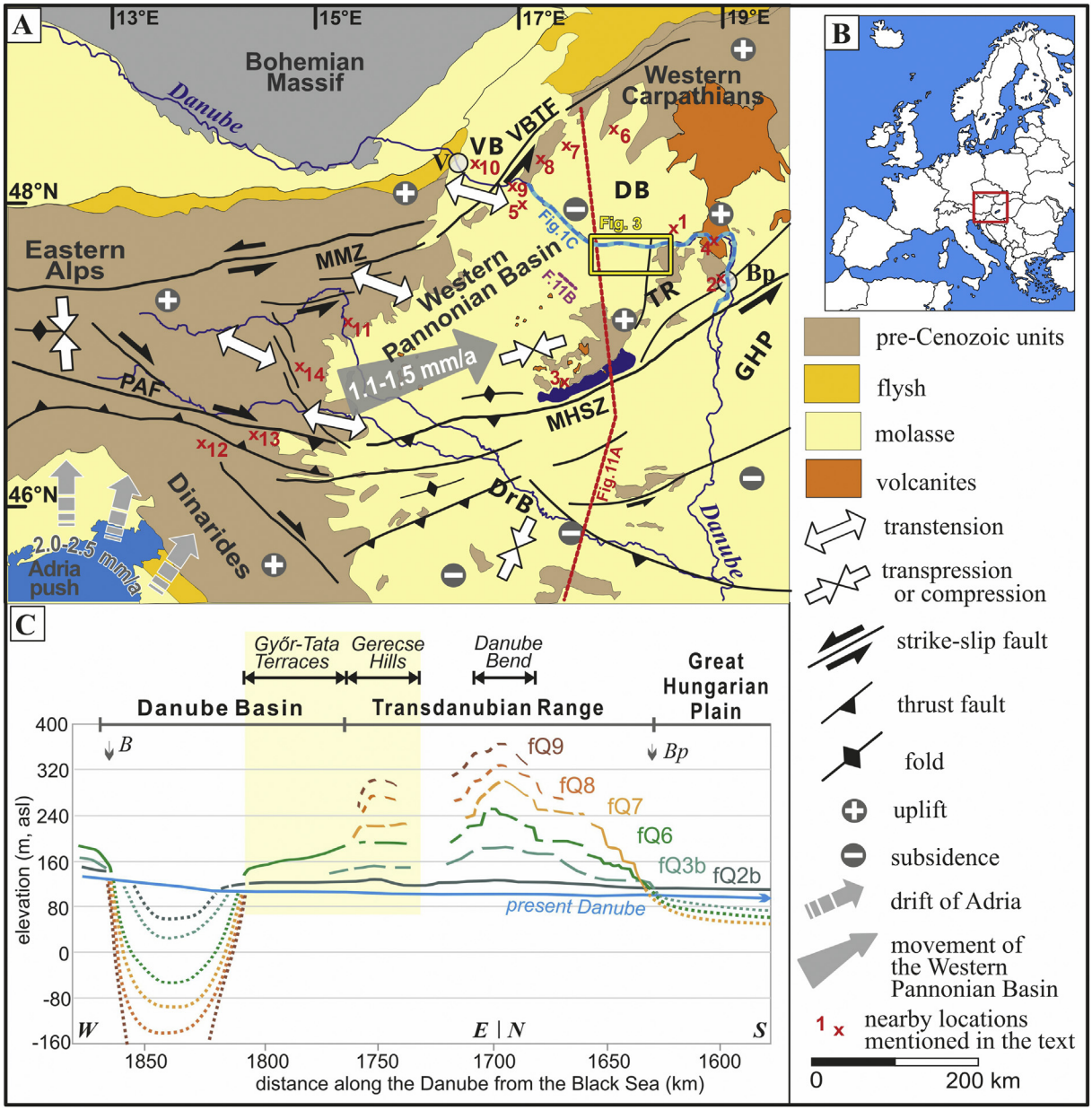

Fig. 1. (**A**) Present-day tectonics of the western part of the Pannonian Basin after Bada et al. (2007). Ongoing northward motion of the Adriatic microplate ("Adria push", 2.0–2.5 mm/a) results in 1.1–1.5 mm/a ENE directed movement of the Western Pannonian Basin unit towards the relatively stable Western Carpathians to the northeast (Vrabec et al., 2006; Bus et al., 2009). Simplified fault pattern after Fodor et al. (2005) and Bada et al. (2007). V: Vienna, Bp: Budapest, VB: Vienna Basin, DB: Danube Basin, GHP: Great Hungarian Plain, TR: Transdanubian Range, DrB: Drava Basin PAF: Periadriatic Fault, MHSZ: Mid-Hungarian Shear Zone, MMZ: Mur–Mürz Fault, VBTF: Vienna Basin Transform Fault. Locations: 1: Nová Vieska; 2: Buda Hills; 3: Balaton Highland; 4: Danube Bend; 5. Nickelsdorf; 6. Veľké Ripňany; 7. Trnava; 8: Stará Garda Cave; 9:Hainburg Hills; 10:Schlosshof and Gaenserndorf terraces; 11: Caves of the Central Styrian Karst; 12: Udin Boršt; 13: Snežna jama; 14: Koralpe. (**B**) Location of Fig. 1A in Europe. (**C**) Longitudinal sketch of some representative terrace levels along the Danube river (modified after Pécsi, 1959). Dotted lines indicate subsurface horizons. Upwarped pattern of the terraces is indicative of surface uplift. Yellow shadow shows the study area. For location see light blue coloured section of the Danube river on Fig. 1A. (For interpretation of the references to colour in this figure legend, the reader is referred to the web version of this article.)

The Danube is the only river cutting through the TR, with the highest preserved terrace levels at ~180 m above the present floodplain. Accordingly, the terraced valley of the Danube river provides a unique opportunity for the quantification of uplift-related incision rates because the incising Danube River is not sensitive to global sea level changes due to its intracontinental setting (Ruszkiczay-Rüdiger et al., 2005a; Gábris and Nádor, 2007; Matenco et al., 2016). The incision rates are quantified using the robust terrace chronological dataset provided by Ruszkiczay-Rüdiger et al. (2016 and 2018). The quantified terrace chronology relies on the combined application of multiple dating methods like cosmogenic radionuclides (CRN), optically stimulated luminescence (OSL) and revised paleontological data.

Aiming at a better understanding of the driving forces of the vertical deformation of the Pannonian lithosphere a high resolution seismic reflection profile along the Danube River is studied. The structures occurring on the profile are constrained by surface structural and borehole data (Csillag et al., 2018; Fodor et al., 2018) and enable the identification of the style of structural deformation and of the magnitude of faulting contributing to the observed deformation. By the synthesis of the estimated incision rates, surface structural and shallow

seismic data, this study contributes to the assessment of the leading tectonic and deeper geodynamic processes that control ongoing kilometre-scale differential vertical movements in the Pannonian Basin.

2. The study area

2.1. Geological background

Formation of the Pannonian Basin was controlled by the eastward retreat of the Carpathian arc. It started about 20 Ma ago, and resulted in the extrusion and rotation of crustal or lithospheric blocks from the Alps and Dinarides (Ratschbacher et al., 1991; Maţenco and Radivojević, 2012; Horváth et al., 2015). Back-arc extension led to the formation of a series of Miocene extensional half-grabens and pull-apart basins (Tari, 1994; Fodor et al., 1999). (Fig. 1; Balázs et al., 2017). Syn-rift faulting and half-graben formation ceased diachronously across the Pannonian Basin, in late Middle and in early Late Miocene times in the western and eastern basin parts, respectively (Fig. 1; Tari, 1994, Balázs et al., 2017).

Late Miocene basin evolution is connected to the development of the large, brackish, isolated Lake Pannon (from ~11.5 Ma; Magyar et al., 2013). Deep basin facies, shelf slope and deltaic sediments progressively filled the lake. In the case of the Danube Basin up to 600 m paleowater depth has been calculated based on the decompacted height of the shelf-slope clinoforms (Balázs et al., 2018). Subsequently, the Danube Basin and the Gerecse Hills became fluvially dominated about 8.5 Ma ago, and during the subsequent 4 million years the shelf margin of the lake prograded ca. 400 km to the SE across the entire Pannonian Basin (Magyar et al., 2013). Several lines of arguments suggest that the TR was almost completely covered by Upper Miocene deltaic sediments of the Lake Pannon or by the subsequent fluvial deposits (Magyar et al., 2017; Sztanó et al., 2016). By the end of the Miocene, the area was part of an alluvial landscape and uplift of the northern TR started in post-Miocene times (Tari et al., 1999).

The alluvial plain of the Danube Basin is still subsiding, hosting a considerable thickness of Quaternary sediments (~450 m; Šujan et al., 2018). Our study area comprises the Győr-Tata Terrace Region (or Győr-Tata Terraces) and the Gerecse Hills. The slightly uplifted Győr-Tata Terrace Region between the Danube Basin and the TR is still characterised by a lowland landscape with more relief only at its eastern, more elevated and dissected segment (Figs. 1C, 2A, B). The hilly and erosionally dissected region of the Gerecse Hills has steeper topography with outcropping Mesozoic carbonates and Paleogene and Neogene siliciclastic lithologies. The most incised section of the Danube valley in Hungary, the Danube Bend lies at the SW–NE trending axis of the TR (Fig. 1A, C). Accordingly, the terrace remnants mapped along the Danube River show a concave geometry relative to the modern river profile, and they are indicators of subsequent stages of uplift-driven river incision, with higher values towards the axis of the TR (Pécsi, 1959; Gábris and Nádor, 2007; Ruszkiczay-Rüdiger et al., 2005a, 2016) (Fig. 1C).

Tilted Miocene layers along the range margins also refer to differential uplift of the TR relative to the adjacent subsiding sub-basins (Horváth and Cloetingh, 1996). Historical earthquakes (Tóth et al., 2002) and the differentially uplifted position of Upper Miocene sediments (Magyar et al., 2017) may suggest the reactivation of some Late Miocene structures.

2.2. Inversion of the Pannonian Basin

During the Late Miocene the basin-scale geodynamic environment substantially changed from syn-rift extension through post-rift subsidence, to large-scale basin inversion of the Pannonian Basin. This resulted in differential vertical movements, in large-scale contractional structures in its southwestern part and in dominantly strike-slip kinematics elsewhere (Fodor et al., 2005; Bada et al., 2007). Seismic interpretation and structural analysis (Fodor et al., 2005; Horváth et al., 2015; Ruszkiczay-Rüdiger et al., 2007) documented the ongoing differential vertical movements manifested in multi-wavelength folding (Tari, 1994) with a maximum of 1 km of amplitude taking into account the effects of differential compaction (Balázs et al., 2018). The onset of positive structural inversion is considered diachronous in different parts of the Pannonian Basin, migrating in time from its Adriatic margin towards the basin centre (Tari et al., 1999; Fodor et al., 2005; Ustaszewski et al., 2014; Maţenco et al., 2016). This pattern is primarily controlled by the counter-clockwise rotation and northward movement of the Adriatic microplate towards the Alpine and Dinaridic margins of the Pannonian Basin (Fig. 1A, Tomljenović and Csontos, 2001; Vrabec and Fodor, 2006). This compression is transferred towards the thinned and weak Pannonian crust (Bada et al., 2007). The Danube Basin and the Great Hungarian Plain shows continuous subsidence. An unconformity is observed near the boundary of the Miocene and Pliocene in the entire Pannonian Basin (e.g., Sacchi et al., 1999; Horváth et al., 2015), between 5 and 6 Ma in the Danube Basin (Šujan et al., 2016). This unconformity, being angular and locally erosional near the basin margins and passing to a correlative conformity towards the basin centre, is related to the onset of basin-scale inversion but the entire process is lasting until recent times. The uplift of the basin margins and the TR caused local erosion and sediment re-distribution towards the subsiding basins. The post-6 Ma differential vertical movements are indicated by sediment thickness values and stress-field modelling (Rónai, 1985; Bada et al., 2007; Kronome et al., 2012; Šujan et al., 2018). According to GPS velocities, the recent shortening rate is 1.3 ± 0.2 mm/a in the western Pannonian Basin, between the Eastern Alpine foothills and the Danube Bend area (Bus et al., 2009; Fig. 1).

2.3. Post Middle Miocene structural evolution of the Gerecse Hills

The Late Miocene deformation was controlled by an extensional stress field with E–W to NW–SE minimal stress axis (Bada et al., 1996; Fodor et al., 1999; Sipos-Benkő et al., 2014). This stress field with normal or oblique-normal slip reactivated all faults with NNW–SSE to NE–SW strike inherited from Jurassic to middle Miocene deformation phases (Fodor et al., 2018). Such faults showing curved traces and anastomosing geometry were mapped on the surface or inferred from borehole data west from the Által-ér creek (Budai et al., 2018). Surface observations, and interpreted seismic sections from the Danube Basin demonstrate that these faults resulted in paleotopographic and facies differentiation (Magyar et al., 2017; Sztanó et al., 2016). These faults clearly post-date the main syn-rift faulting and graben formation of the Danube Basin, but their origin remains enigmatic.

The faulting has diverse time constraints, depending on the stratigraphic composition of the footwall and hanging wall; this is reflected in the colour code of Fig. 3. Variable observations, including abrasional gravel, small sedimentary dykes (Fodor et al., 2018), one possible paleotsunami (Sztanó et al., submitted), and sediment transport direction (Bartha et al., 2015) demonstrate syn-sedimentary Late Miocene activity of the range-bounding fault system of the Gerecse Hills; this faulting occurred between 9.4 and 8.7 Ma (Magyar et al., 2017).

Nevertheless, several faults cut through the entire Upper Miocene sequence. In this case, the lower time constraint for fault slip is given by the youngest deposits in the hanging wall. When only a thin sequence is present, and the footwall is composed of pre-Miocene rocks, faulting could start as early as ~9.4 Ma. When the hanging wall has the complete Miocene stratigraphy, faults were still active after the deposition of the last Upper Miocene units, locally deposited between 8.7 and 8.0 Ma (Magyar et al., 2017). Just north of the Gerecse Hills, across the Danube the youngest, slightly faulted fluvial sediments were deposited around 7 Ma. In other parts of the Danube Basin post-rift sediments accumulated under the same conditions up to 6 Ma (Šujan et al., 2020). Thus all the mapped faults were active either during the Late Miocene (~9.4–6 Ma) or during the neotectonic deformation, which started

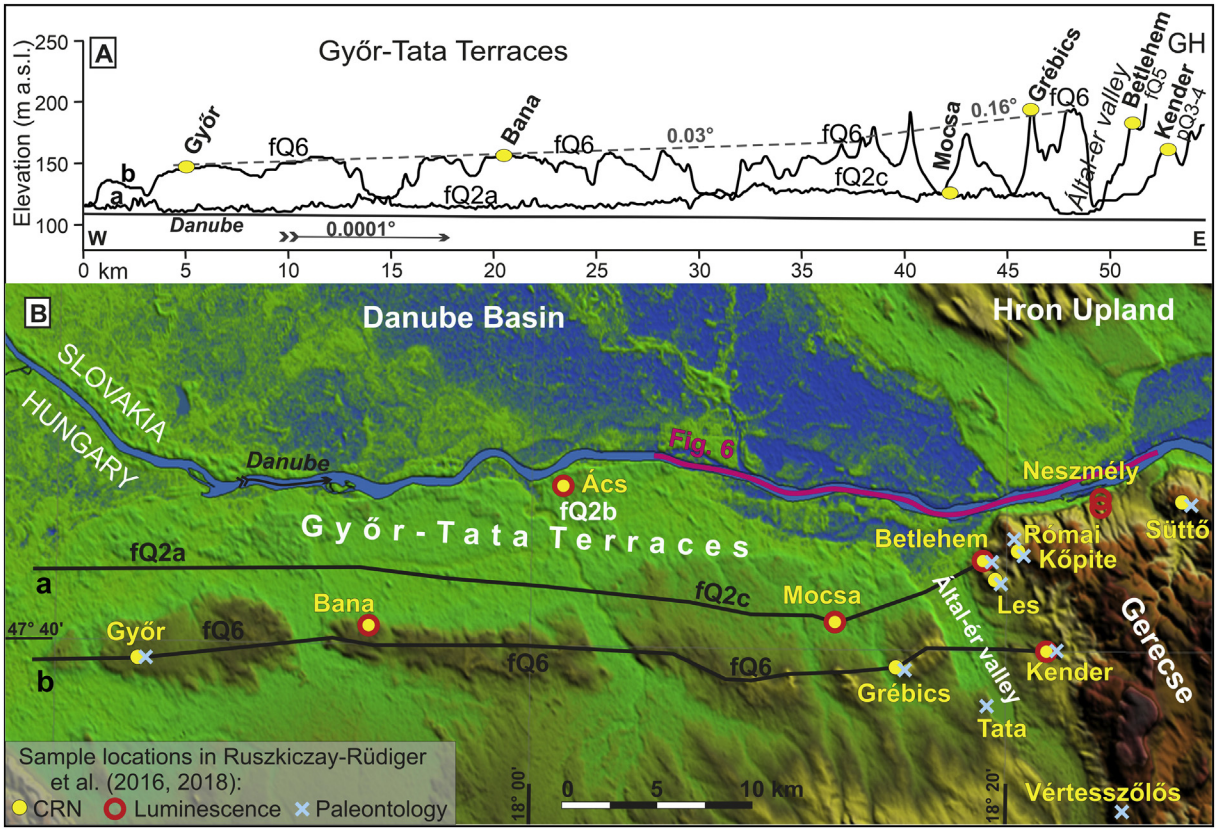

Fig. 2. (A) Longitudinal profiles representing the position of the fQ2a and fQ2c (a), and the fQ6 (b) terraces along the Danube in the Győr-Tata Terrace Region. Yellow dots are sampled locations studied by Ruszkiczay-Rüdiger et al. (2016, 2018). Grey dashed line is the envelope slope of the fQ6 terrace. GH: Gerecse Hills. (B) Digital elevation model of the study area, with the locations used for age determination (Ruszkiczay-Rüdiger et al., 2016, 2018). The pink line is the path of the seismic reflection profile of Fig. 6. Black lines a and b show the locations of the profiles which appear on inset A. (For interpretation of the references to colour in this figure legend, the reader is referred to the web version of this article.)

around 6 Ma (Bada et al., 2007; Horváth et al., 2015).

The numerous travertine deposits, ranging in age from Late Pliocene to Quaternary, could also indicate the location of active deformation at the time of carbonate precipitation (Fig. 3A; Pécsi et al., 1982; Kele, 2009; Sierralta et al., 2010; Török et al., 2017, 2019). Except for the well-studied Süttő locality, where clear sign of active faulting, namely a WNW-trending fissure ridge has been demonstrated (Török et al., 2019), detailed structural data are missing, and the mapping work did not prove clear sign of Quaternary deformation. For instance, closely orthogonal sediment-filled fractures could derive either from tectonic faulting or from surface processes, like sliding (Török et al., 2017). In all other outcrops Quaternary deposits are non-faulted, although the presence of Quaternary deformation could not be excluded due to poor outcrop conditions.

The recent stress field is different from the Miocene one; the regional stress-field data (Bada et al., 2007) and few nearby earthquake focal mechanism solutions (Madarás et al., 2012; Wéber and Süle, 2014; Hók et al., 2016; Wéber, 2016) suggest strike-slip type deformation with NE–SW compression and perpendicular extension. The change in the stress field is not well constrained but thought to be connected to the onset of neotectonic deformation around the Miocene-Pliocene boundary. The neotectonic stress field would have induced new kinematics on the Late Miocene to Pliocene faults; dextral and reverse slip on N−S and NW–SE striking faults, respectively.

2.4. Terraces of the Danube in Hungary

The terraces of the Győr-Tata Terraces and the Gerecse Hills form a coherent system at subsequent river sections (Pécsi, 1959; Ruszkiczay-Rüdiger et al., 2005a), thus terrace age-elevation datasets can be integrated and discussed together. The terraces in Hungary are numbered from fQ1 (lowest) to fQ9 (highest), and form up to 11 levels; Csillag et al., 2018, Ruszkiczay-Rüdiger et al., 2018). In the Győr-Tata Terraces, terrace levels have developed up to horizon fQ6, but the terrace sequence is not complete. The fQ6 terrace appears as a train of flat-top, gravel-covered mounds. This terrace is clearly oppositely tilted compared to the present-day Danube profile: the relative elevation of the fQ6 terrace, shows a gradual increase from west (~37 m above the Danube) to east (~96 m), from the Danube Basin towards the Gerecse Hills (Fig. 2A,B).

The most complete terrace staircase in the Hungarian Danube valley has developed in the Gerecse Hills, with the valley floor at 103 ± 1 m a.s.l. and the highest level at ~285 m a.s.l. (fQ9), Table 1, Fig. 3). The terraces are frequently covered by travertine deposits of up to 30–40 m in thickness. Travertines often display spring-mounds and ponds of lacustrine environment (Scheuer and Schweitzer, 1988; Kele, 2009; Török et al., 2017). On the northern side of the Danube (Hron Upland, Slovakia, Fig. 2), opposite the Gerecse Hills up to 6 terrace levels could be described with a relative height of ~80 m for the highest terrace (Šujan and Rybár, 2014).

In the Danube Bend the Danube is incising into Miocene volcanic rocks (Fig. 1A; Ruszkiczay-Rüdiger et al., 2005a) and formed a staircase of terraces with the highest elevations differences up to the fQ9 level. At this valley section the terraces above the fQ2c level are mostly uncovered strath terraces.

In this study terrace age-elevation data pairs published by Ruszkiczay-Rüdiger et al. (2016 and 2018) are used to quantify river incision and related surface uplift rates in this area. This terrace-

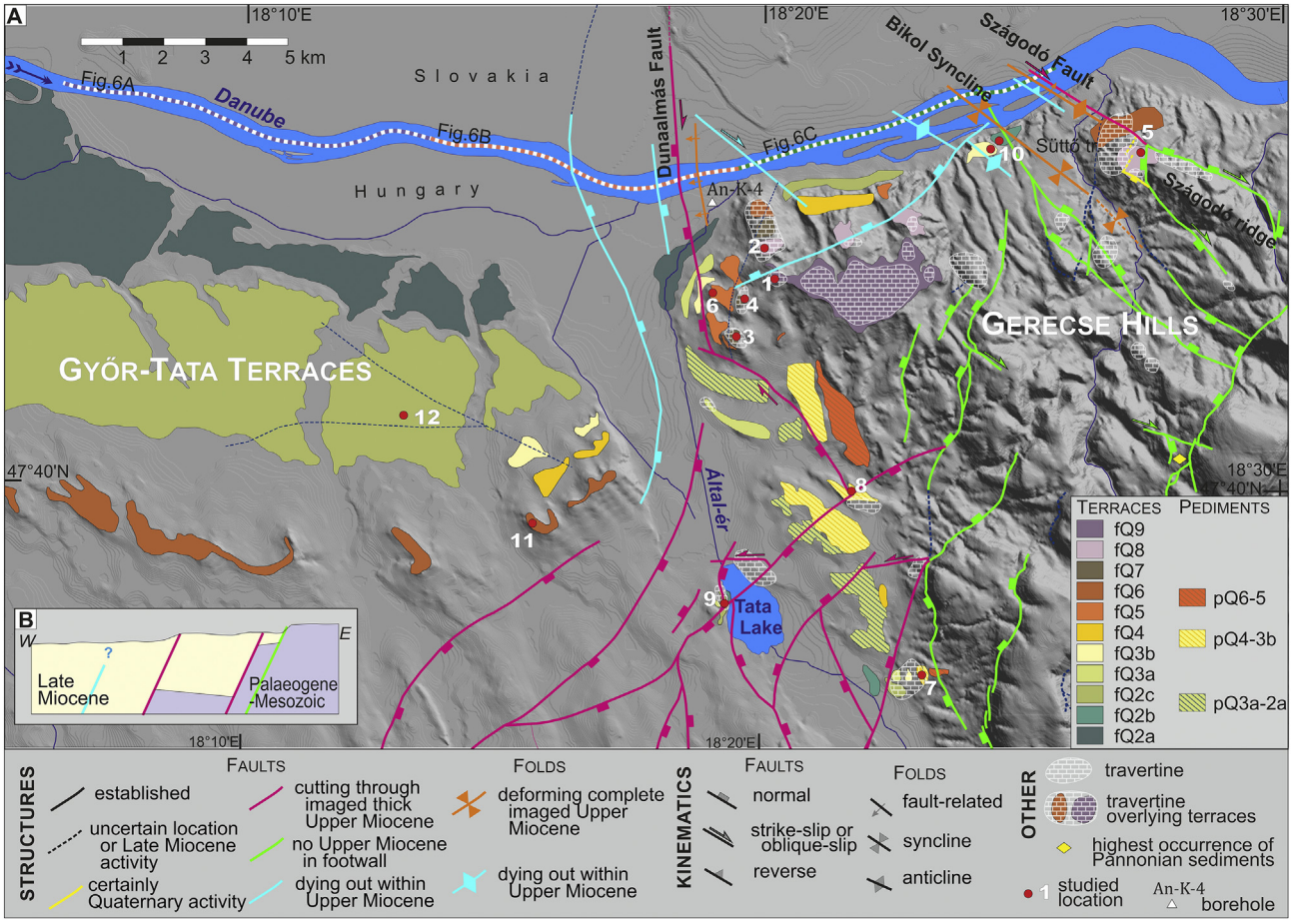

Fig. 3. (A): Digital elevation model of the eastern Győr-Tata Terraces and western Gerecse Hills with the terraces and studied locations (Ruszkiczay-Rüdiger et al., 2016, 2018). 1: Kőpite Hill, 2: Roman Quarry, 3: Les Hill; 4: Csúcsos Hill, 5: Süttő, 6: Betlehem Quarry, 7: Vértesszőlős, 8: Kender Hill, 9: Tata, 10: Neszmély. 11. Grébics Hill, 12. Mocsa. Late Miocene fault pattern with possible post-Miocene reactivation, (after Fodor et al., 2018, revised by this study). Position of the multichannel seismic survey along the Danube is indicated by dotted lines (Fig. 6A-C). Travertine occurrences are outlined after Scheuer and Schweiter, (1988) and Budai et al. (2018). Note that downstream from the Tata Lake the present day Által-ér creek flows in an artificial channel. **(B)** Explanatory sketch showing the colour code for different fault types mapped on Fig. 3A. For colours the reader is referred to the web version of this article.

chronological dataset relies on in situ produced cosmogenic ^{10}Be depth profiles and ^{26}Al/^{10}Be burial durations and on optically stimulated luminescence dating (OSL, in most cases the post-IR IRSL (pIRIR$_{290}$) method was applied). The numerical ages were compiled with revised paleontological ages and were compared to published magnetostratigraphic and U-series data of travertines covering the terraces (Ruszkiczay-Rüdiger et al., 2016 and 2018). The studied locations appear in Figs. 2 and 3. Terrace elevation and age data with references are summarized in Table 1 and in Fig. 4. More detailed description is in Supplementary material 1, section S1 and Supplementary material 2, Table S1.

3. Methodology

3.1. Multichannel seismic survey

High-resolution multichannel seismic profiles were measured on the Danube River on its W–E trending section between 17.82° E and 18.73° E in 2008. This method is particularly suitable to image the sedimentary layers and structures within the uppermost 300–500 m below the surface with a vertical resolution of ~12 m (6–16 m). The reflectivity and signal to noise ratio of the seismic data substantially decreases beneath the Late Miocene unconformity, thus our interpretation is focused on the Miocene to Quaternary sedimentary basin fill.

Seismic data acquisition was carried out using the marine surveying instruments of Delft University of Technology, the Netherlands. A 20 cu-inch airgun was used as a source and a 24-channel streamer with 3.125 m hydrophone interval was towed behind the ship. Seismic data processing was carried out at Eötvös Loránd University in Hungary and followed the standard processing steps, such as bandpass filtering (0–30–90–9150 Hz), FK filtering, spiking deconvolution, normal moveout correction and stacking. Here we present a 27 km-long seismic section, located to the north of the eastern Győr-Tata Terraces and western Gerecse Hills and displayed in two-way travel time with an approximate vertical exaggeration of 24 (Fig. 6).

3.2. Quantification of incision rates

Although slightly different aspects of the incision are documented by the diverse chronological tools, together they determine the incision rate of the Danube quite well. Chronological data derived directly from the terrace material are relevant to the deposition and subsequent burial of the terrace (CRN burial durations, OSL and paleontological ages) or refer to the time of terrace abandonment (CRN depth profile ages). The age of travertines overlying terrace sediments provides a minimum age constraint to terrace abandonment, and can thus be used to estimate maximum incision rates. Similarly, minimum terrace ages allow for the determination of maximum incision rate.

The sample locations and the position and elevation of the terraces are reported in accordance with Ruszkiczay-Rüdiger et al. (2016, 2018)

Table 1
Terrace chronological data of the Hungarian Danube valley.

Stage	Terrace label	Terrace label before 2018		Elevation of terrace surface (m, a.s.l.)	Elevation of terrace base (m, a.s.l.)	Terrace age (ka)	Age of terrace cover (ka)	Age determination method	Best constrained time range of terrace formation(ka)	Marine Isotope Stages	Best constrained incision rate**
Pliocene	fQ9	tVII		273–285	265–270	2942 ± 486	7000–2000	paleontology, v.[2] CRN burial duration[2]	***3428–2456***	MG 5–MIS 97	50–70
Early Pleistocene	fQ8	tVI		255–270	240–250		2600–1950	paleontology, v.[2]	***~2600–2200***	MIS 104–84	< 57–67
	fQ7	tV		216–232	214–220	2400–2000 2323 ± 140		paleontology, v.[2] CRN burial duration[2]	***2400–2183***	MIS 94–83	49–56
	fQ6			191–205	190–200	> 1000 1900–1100		CRN depth profile[1a] paleontology, g.[2]	***1900–1100***	MIS 71–33	43–74
	fQ5	tIV		171–185	170–178	1100–780 > 713 > 365		paleontology, g.[2] CRN depth profile[2] pIRIR$_{290}$[2]	***1100–780***	MIS 32–20	71–100
Middle Pleistocene	fQ4			160–165	155–160		500–400	paleontology, v.[2]	***~600–424***	MIS 14–12	108–153
	pQ4-3b			~157*	~153*	650–130 $404^{+248}/_{-168}$ 471 ± 41		paleontology, g.[2] CRN depth profile[2] pIRIR$_{290}$[2]	***512–430***	MIS 13–12	114–140
	fQ3b	tIII	tIIIb[4]	145–155	140–150	301 ± 32 to 264 ± 26		pIRIR$_{290}$[2]	***333–238***	MIS 9–8	141–197
	fQ3a			133–138	132–135			no data	***~250–150***	MIS 7–6	141–175
	fQ2c	tIIb	tIIIa[4]	125–132	120–125	143 ± 10		pIRIR$_{290}$[1]	***153–133***	MIS 6	193–222
							130–90	paleontology, v.[2]			
Late Pleistocene	fQ2b		tIIb[4]	118–121	114–115	91 ± 6 117 ± 9 to 98 ± 7		pIRIR$_{290}$[1] pIRIR$_{290}$[2]	***126–85***	MIS 5e–b	175–241
	fQ2a	tIIa		113–116	107–110		14.8–13.6 14.1 ± 2.3; 16.0 ± 2.0	^{14}C[3] TL; IRSL[3]	***~70–14***	MIS 4–2	221–1107
Holocene	fQ1b	tIb		104–108	91–96	recent			***12–0***	MIS 1	
	fQ1a	tIa		103–104	90–95						

Former terrace labels after Pécsi (1959) for more details refer to Ruszkiczay-Rüdiger et al. (2005a). The terrace surface and base elevations are valid for the Gerecse Hills (after Csillag et al., 2018; Ruszkiczay-Rüdiger et al., 2018). MIS stages after Lisiecki and Raymo (2005). * interpolated terrace elevation values from previous and subsequent terraces in the Danube valley; ** the best constrained uplift rates referring to the Gerecse Hills section of the valley, calculated using the mean terrace base elevation; [1]: Ruszkiczay-Rüdiger et al. (2016); [1a]: Ruszkiczay-Rüdiger et al. (2016) revised by this study; [2]: Ruszkiczay-Rüdiger et al. (2018); [3]: Ujházy et al. (2003), here the dated formation is a terrace covering aeolian sand; ^{14}C data were recalibrated using IntCal13 (Reimer et al., 2013); [4]: earlier subdivision of the former tIII and tII levels (Gábris and Nádor, 2007; Gábris et al., 2012; Ruszkiczay-Rüdiger et al., 2016); paleontology, v.: vertebrate data, g.: gastropod data. For names and coordinates of the dated locations Refer to Table S1a, b and c, Fig. 2B,3A. For an overview of terrace positions and ages see Fig. 4.

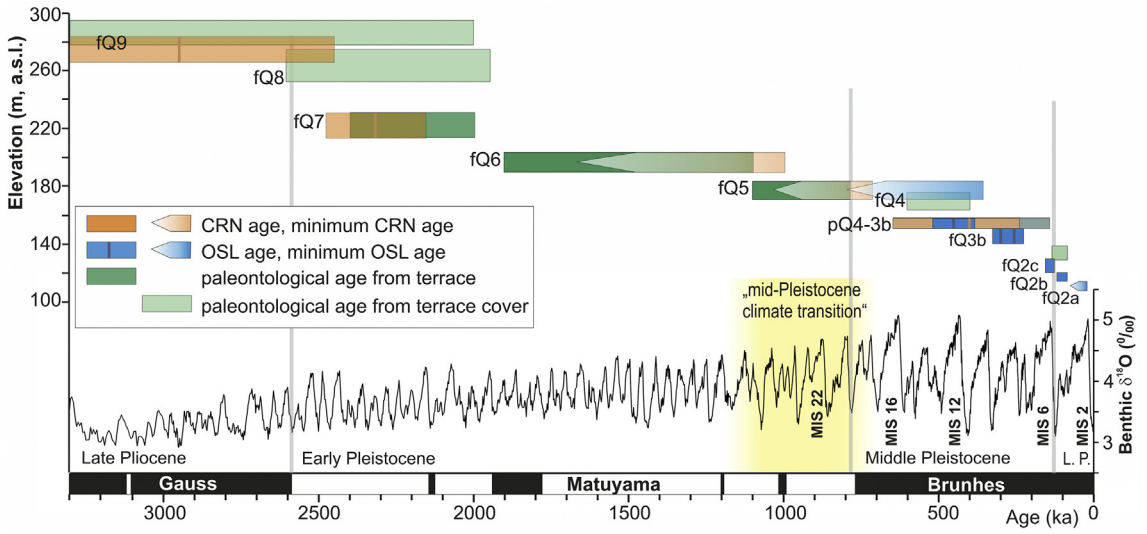

Fig. 4. Periods of terrace formation in the northern TR in the Danube valley according to CRN, OSL and paleontological data plotted in function of the terrace elevation. Rectangles represent the age and elevation range covered by the terrace and overlying travertine levels. The data and references appear in Table 1. MIS stages after Lisiecki and Raymo (2005). Geomagnetic timescale after Cohen and Gibbard (2016). For colours the reader is referred to the web version of this article.

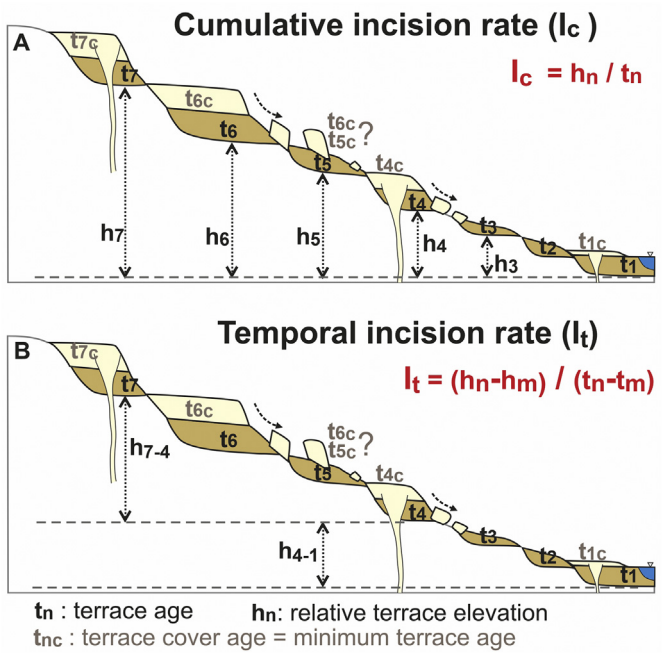

Fig. 5. Geometry and relevance of numerical ages of terrace-related sediments to quantify the rate of river incision. (A): Determination of the cumulative incision rate. (B): Basic concept of the determination of the temporal incision rate. For the calculation of the temporal incision rates all relevant age-elevation data-pairs were considered (see details in the text). Note that the cross section is not to scale and number of terraces is fewer than in the study area. For colours the reader is referred to the web version of this article.

(Tables 1, S1B, Fig. 4). The elevation of the base of the terrace material at each level and the base of the present day Danube alluvium as reference level (~93 m a.s.l. at the Gerecse Hills and 95–97 m at the Győr-Tata Terraces) were used for the calculation of the incision rates (Tables 1, 2, S1, Fig. 5). The elevation of the base of the terraces was determined using borehole and field data (Csillag et al., 2018). In the Által-ér valley (tributary of the Danube, incised between the Gerecse Hills and the Győr-Tata terraces, Figs. 2, 3), the elevations of dated pediments, terraces and related travertines were converted to the elevation values of the relevant Danube terraces to exclude anomalies related to local base-level differences. This normalised dataset was used during the quantification of the incision rates in the study area.

Two approaches were applied for the calculation of the incision rates:

1) The cumulative incision rate corresponds to the incision rates averaged over the entire timespan defined by the terrace age and its elevation above the river (Fig. 5A). This method enables comparison with published incision/uplift rates covering similar periods of time. However, it may integrate periods with different incision rates and does not allow to recognise their temporal variations.
2) The temporal incision rates are calculated for certain time-slices of the incision history to exclude artefacts of integrating over periods of different incision signals (Fig. 5B). These calculations are possible only when the terrace record is detailed enough for the identification of possible breakpoints in the uplift history. For this purpose, the terrace-chronological data are merged in order to obtain an age–elevation data pair with uncertainties for each terrace level (Table 2).

In order to find the best fit incision rate for the integrated age-elevation dataset the linear, least-squares fitting was applied (Williamson-York bivariate fitting; Cantrell, 2008). This method is suitable for estimating the best fit straight line to data accounting for uncertainties present in both the x and y variables (age and elevation uncertainties). When the linear fit is successful for certain set of age-elevation data pairs, its slope is equivalent to the incision rate relevant to that period of time.

4. Results

4.1. Structural interpretation of the seismic section

The high-resolution seismic profile (Fig. 6), measured from the Gerecse Hills (east) and the Danube Basin (west), shows the characteristic tectonic features of this transitional zone. Late Miocene sediments are uniformly tilted towards the Danube Basin (Fig. 6A). These sediments are affected by a series of faults with small normal offsets (ca 20 m). Late Miocene horizons are onlapping on a marked unconformity separating the Late Miocene and underlying pre-Miocene clastics and/or Mesozoic rocks while the higher reflections are erosionally truncated towards the east. Two high-angle faults are visible in the centre of the

Table 2
Simplified, merged age-elevation data of the terraces in the Gerecse Hills used for temporal uplift rate calculations.

Terrace label	Mean elevation of terrace base (m, a.s.l.)	Uncertainty (m)	Mean age (Ma)**	Uncertainty (Ma)	Mean cumulative uplift rate (m/Ma)	Uncertainty plus (m/Ma)	Uncertainty minus (m/Ma)
Gerecse Hills							
fQ9	267.5	2.5	2.94	0.49	59	+12	−8
fQ8	245	5	2.40	0.20	63	+6	−5
fQ7	217.5	2.5	2.29	0.11	54	+3	−2
fQ6	195	5	1.50	0.40	68	+25	−14
fQ5	174	4	0.96	0.13	84	+18	−12
fQ4	158	5	0.51	0.10	127	+26	−19
pQ4-3b	153	5	0.47	0.04	127	+12	−10
fQ3b	145	5	0.29	0.05	181	+36	−26
fQ3a	133.5	1.5	0.20*	0.05*	203*	+68	−41
Győr-Tata Terraces							
fQ6 west	134	2.5	1.5	0.4	29	+11	−6
fQ6 middle	145	2.5	1.5	0.4	37	+13	−8
fQ6 east	190	2.5	1.5	0.4	67	+24	−14
Both areas							
fQ2c	122.5	2.5	0.14	0.01	206	+16	−13
fQ2b	114.5	0.5	0.11	0.02	204	+49	−33
Base of Danube alluvium	93	3	0.00	0.00			

*No age data are available; the tentative ages were calculated using the extrapolation of the ages from the subsequent terrace levels. These numbers are not considered for the calculation of temporal incision rates.

section within the Late Miocene sediments. Further to the east, near the borehole An-K-4 a westward dipping Late Miocene moderately dipping normal fault cutting through the imaged Late Miocene package (Dunaalmás Fault) and a smaller offset antithetic fault are present (Figs. 3, 6B).

Late Miocene–Quaternary sediments in the eastern part of the section (Fig. 6C) show a synclinal geometry and onlap on the flanks of the underlying top-Paleogene unconformity, a structure called here as the Bikol Syncline. Two small-offset pop-up structures create gentle anticline geometries within the Late Miocene sediments and other steep faults also occur; the lowermost Upper Miocene reflectors either cover the structures or onlap on their sides.

In the easternmost part of the section, horizons are elevated above a basement high cross-cut by a series of high angle faults (Fig. 6C); it is named here as Ságodó Fault Zone or Ságodó Ridge. The fault zone seems to have a complex architecture on the seismic line; north-dipping, steep reverse fault in the south, sub-vertical, potentially strike-slip fault branches in the core, and north-dipping apparently normal fault at the northern boundary. Altogether, fault branches create a fault-related antiform (Figs. 3A, 6C) reflected on the base-Miocene surface.

4.2. Correlation of structures below the Danube and in the Gerecse Hills

The Dunaalmás Fault near the borehole An-K-4 can be correlated to the map-scale faults depicted on earlier maps (Fodor et al., 2018; Fig. 3A). Borehole data demonstrate that this fault has considerable displacement in the pre-Cenozoic level; it represents the western boundary fault of the Gerecse Hills.

The next structure to the east of the An-K-4 borehole is difficult to correlate to any of the faults mapped in the Gerecse Hills. It is probably a strike-slip fault terminating against another fault, running towards ENE. The small anticline on the pre-Late Miocene surface at 22–23 km (Fig. 6C) is interpreted as a transpressional strike-slip and can be followed towards the southeast in the Gerecse Hills, where the top of Cretaceous seems to depict an antiform (near sample site nr. 10 on Fig. 3A). All these structures die out within the Late Miocene sequence.

The Bikol Syncline recognised on the seismic section can be connected to a similar structure further to the southeast. The topographically lowest zone of the syncline is occupied by Paleogene and Late Miocene sediments, while these were mostly eroded from the more elevated eastern parts. The nature of this structure differs along strike; it was interpreted as a northwest-trending graben in the southeast, but it seems to be more like a faulted syncline below the Danube.

The Ságodó Fault zone and the associated morphological ridge cutting the eastern end of the seismic section continues south-eastward. On both sides of the ridge the stratigraphy is similar; Mesozoic is covered by Paleogene and Late Miocene sediments. The displacement increases east from the Süttő travertines, where a N−S trending cross fault displaces Late Miocene against Cretaceous rocks.

4.3. Incision rates and their spatial and temporal patterns

4.3.1. Cumulative incision rates

In the Győr-Tata Terraces cumulative incision rates vary between ~19 and ~86 m/Ma (Table S1b) for the highest, fQ6 level, being relevant during the last 1.5 ± 0.4 Ma. Incision rates show a decreasing trend towards the subsiding Danube Basin (spatial changes of incision rates are discussed in section 5.2). Incision rates for the younger terraces fQ2c and fQ2b reach values as high as ~200 m/Ma, relevant for the last ~140 ka (Table 2).

In the Gerecse Hills, the terrace-chronological data enabled the estimation of cumulative incision rates for terraces older than 1 Ma in the range of from ~50 to ~70 m/Ma. Over the last ~1.0 Ma cumulative incision rates show an increasing trend up to ~200 m/Ma (Figs. 7, Tables 1, 2), similarly to the Győr-Tata Terraces. However, this gradual increase of the incision rates might be a bias due to higher incision rates of the younger terraces integrated in the cumulative rates for longer timespans. Accordingly, it is important to study different time slices of the incision history to reveal possible temporal changes of the incision rates.

4.3.2. Temporal incision rates

Fitting a trend-line to the terraces from the fQ9 to the fQ2c level, the resulting incision rate is 51 ± 5 m/Ma for the ~3 Ma–140 ka period in the Gerecse Hills (Fig. 8). In the Győr-Tata Terraces this period is represented by the single west-east trending fQ6 terrace train. Here a simple linear regression was used to estimate the incision rates at the western (Győr) middle (Bana) and eastern (Grébics) sections of this terrace providing incision rates of $9\ ^{+4}/_{-2}$ m/Ma, $17\ ^{+7}/_{-4}$ m/Ma and $50\ ^{+20}/_{-11}$ m/Ma, respectively (green lines on Fig. 8). These rates are relevant for the period between 1.5 ± 0.4 Ma and ~ 140 ka. It is to be noted that cumulative incision rate at the easternmost part of the Győr-

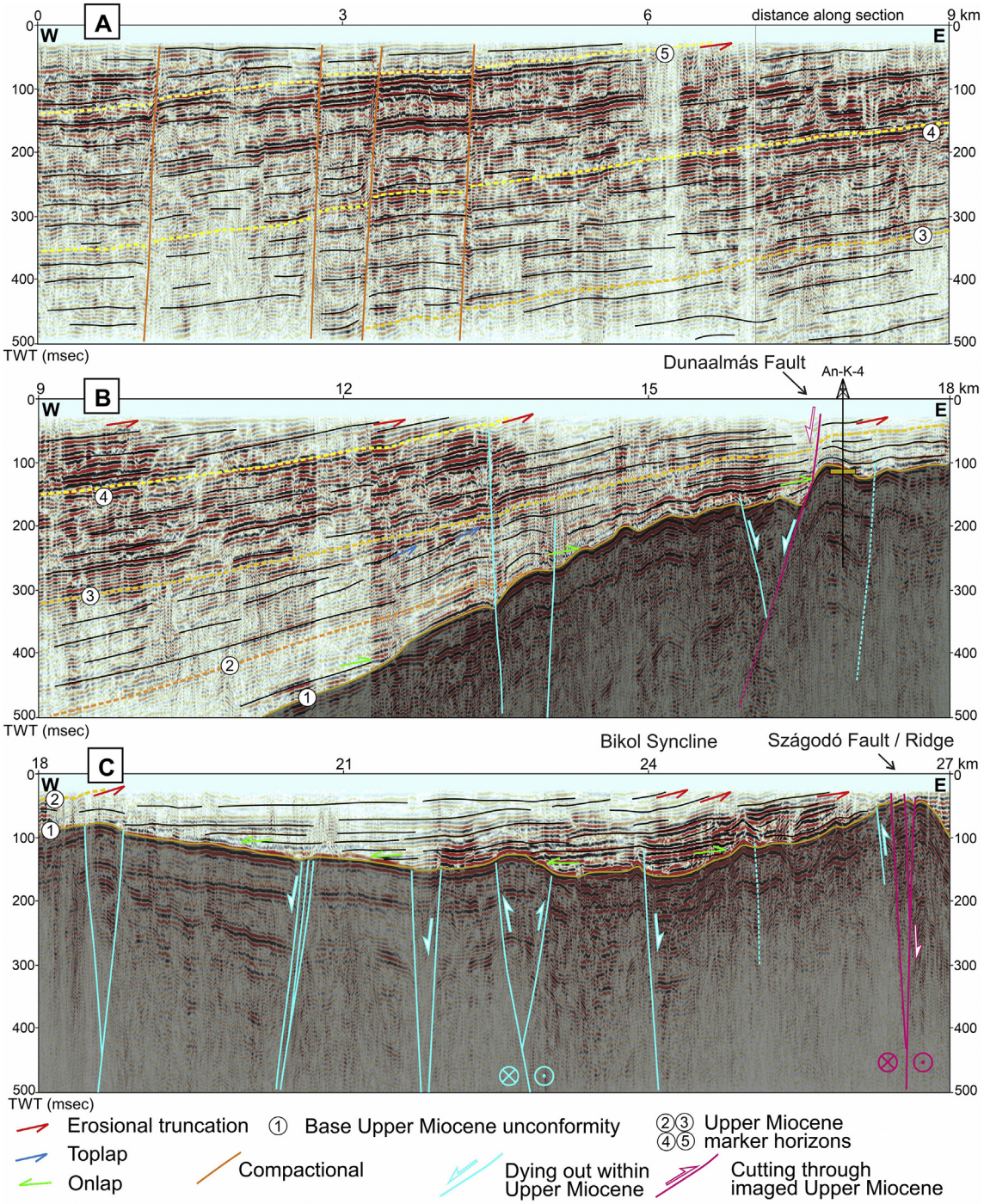

Fig. 6. Interpreted multichannel seismic profile measured on the Danube River in the proximity of the Győr-Tata Terraces. For location see Figs. 2B, 3A. Seismic profile is highly vertically exaggerated (ca. 24×). The base Upper Miocene (Pannonian) unconformity (yellow horizon no. 1) is constrained by well data (An-K-4). Note the erosional truncation of the Late Miocene marker horizons towards the Gerecse Hills (red arrows). (For interpretation of the references to colour in this figure legend, the reader is referred to the web version of this article.)

Tata Terraces during this time interval is indistinguishable from that of the Gerecse Hills.

During the last ~140 ka a fourfold increase (to 207 ± 1 m/Ma; Fig. 8) of the uplift rate can be calculated both in the Gerecse Hills and in the western Győr-Tata Terraces.

5. Discussion

5.1. Structural deformation

The seismic section along the Danube complete our knowledge on the age of deformation in the western Gerecse Hills and their foreland. In the western part of the seismic section the faults belonging to this system clearly die out within the Upper Miocene sequence (Fig. 6B) suggesting their negligible neotectonic activity. East from the An-K-4 borehole, some faults and the initial stage of the Bikol syncline only

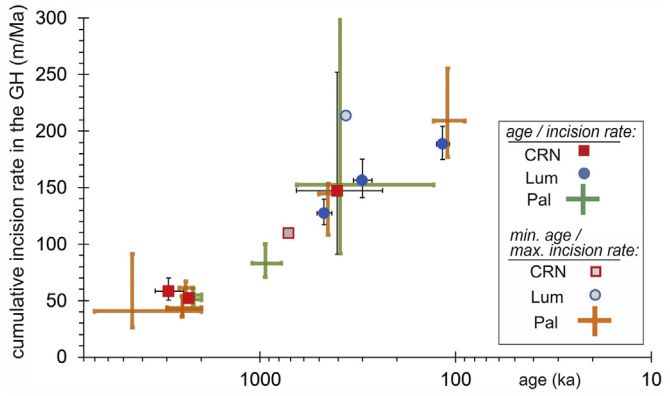

Fig. 7. Terrace ages plotted against the cumulative incision rates in the Gerecse Hills. CRN: Cosmogenic Radionuclide data, Lum: Luminescence data, Pal: Paleontological data. Data are available in Table 1. For colours the reader is referred to the web version of this article.

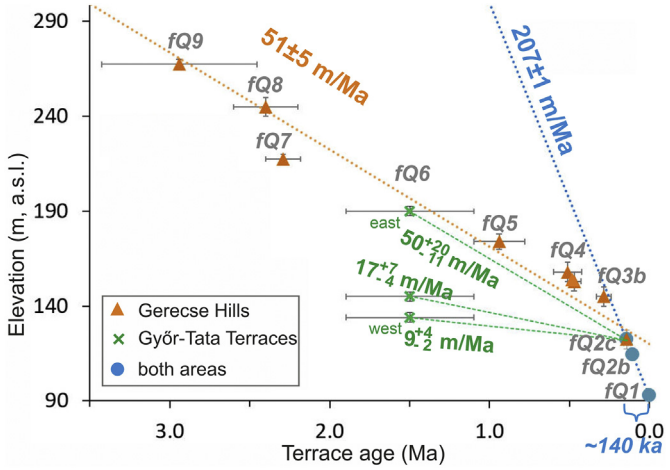

Fig. 8. Temporal uplift rates in the Gerecse Hills and in the Győr-Tata Terraces. For age-elevation data refer to Table 2). Note the gradual increase of uplift rates from west to east in the Győr-Tata Terraces for the fQ6 terrace. For colours the reader is referred to the web version of this article.

slightly deform the base of the Upper Miocene. The oldest Miocene layer has an age of ca. 8.7 Ma, therefore this deformation could be coeval or slightly predate this time and has no neotectonic slip.

The Upper Miocene strata are onlapping on the western limb of the Bikol Syncline, and the same layers are uniformly tilted to the west and truncated by the river on the eastern limb of the fold. Although the west-dipping reflectors could be interpreted as original clinoforms of a west-prograding small slope, this interpretation is unlikely, because no correlative formation has been documented in any cores of the Gerecse Hills. In addition, seismic data and paleogeographic reconstruction suggest the presence of such slope west (basin-ward) from the Gerecse paleohigh (Sztanó et al., 2016) as is seen on Fig. 6. between reflectors 2 and 3. Thus the tilted geometry suggests a pre- and a post-Late Miocene deformation phase; the latter being the case on the eastern limb (Ságodó Ridge). These data point to post-Miocene folding, and the Quaternary age cannot be excluded.

The Dunaalmás and Ságodó Fault zones cut through the entire imaged Miocene sequence and above the Ságodó Ridge the entire Miocene package was homogenously broadly west-tilted (Figs. 3A,B, 6C). The age of this deformation clearly post-dates the youngest preserved sediments of ~8 Ma, but the deformation is not well-constrained; its Plio-Quaternary activity cannot be excluded nor proved. While the Ságodó Fault zone and the Bikol syncline can be followed on the surface, and while they are perpendicular to the recent maximal stress axis, their contractional character is plausibly postulated. The orthogonal fissure ridge and sediment-filled fracture system of the Süttő travertine complex (Török et al., 2019) corroborate Quaternary age of the antiformal Ságodó Ridge. One set of fractures is perpendicular to the structure, (parallel to postulated σ1 maximal stress axis), while the other one is parallel to the ridge and may express local extension on top of the antiformal ridge. Finally, a number of islands occurring in the Danube upstream from the antiformal Ságodó Ridge could be related to its ponding effect (Fig. 3A).

All these observations show that evidence for post-Miocene faulting is scarce both on the seismic line and on the surface. The above described, potentially neotectonic structures did not cause a large (> 100 m) deformation within the entire area. The largest neotectonic deformation feature remains the westward or north-westward tilt (1–2°) of the Upper Miocene strata at the Győr-Tata Terraces and the western Gerecse Hills (Fig. 6A, B), which uniformly affected the entire Miocene suite. The fQ6 terrace train is tilted in similar direction but with smaller value (Fig. 2A) suggesting a latest Pliocene to Quaternary age for the tilt. However, this structure has dozens of km wavelength, much larger than the study area. All the other scarce upper crustal faults and folds do not seem to be large enough to accommodate the differential vertical displacement observed between the western and eastern part of the area.

5.2. Spatial and temporal change of the incision rates

The terrace chronological data supports the reconstruction of two periods of different incision rates. The first period from ~3 Ma to ~140 ka is characterised by an incision rate of 51 ± 5 m/Ma in the Gerecse Hills. Terraces older than 1.5 ± 0.4 Ma (fQ6 terrace) are not present in the Győr-Tata Terraces, therefore until then this area must have been close to base level or subject to bevelling under slow uplift (Bufe et al., 2016). Between ~1.5 Ma and ~ 140 ka, incision rates suggest that uplift was ~5 times faster in the Gerecse Hills compared to the westernmost part of the Győr-Tata Terraces (51 ± 5 m/Ma and 9 $^{+4}/_{-2}$ m/Ma, respectively; Figs. 8 and 9). After ~140 ka incision rates are uniformly fast in the study area (207 ± 1 m/Ma). Unlike it was described for several river systems in Europe (Gibbard and Lewin, 2009), our dataset suggests no significant change in the incision rate in the Gerecse Hills during the time of the mid-Pleistocene climate transition (Clark et al., 2006) (Figs. 4, 8).

At the same time, cumulative incision rates in the Gerecse Hills show a gradual increase with time (Fig.7). In Fig. 9. both temporal rates and cumulative rates for all locations are plotted along the Danube river. For terraces older than ~2 Ma (fQ7-fQ9) the two approaches show similar rates in the Gerecse Hills. During the last 1.5 ± 0.4 Ma (fQ6-fQ3) steadily increasing cumulative incision rates manifest strong influence of the short term, fast incision rate in the Late Pleistocene: the younger is the terrace the closer is its cumulative incision rate to the value relevant for the last ~140 ka. In other words, cumulative incision rates for periods longer than ~140 ka are biased towards faster values due to integrating both the slower, long-term incision rate and the last period of faster incision.

It is an open question whether the acceleration of the incision during the last ~140 ka is a result of an acceleration of uplift or it is a rate biased by a short-term, climate-triggered incision event temporally exceeding the pace of rock uplift (as suggested by DiBiase, 2014). This period coincides with the last glacial cycle, and is shorter than the time gap between most of the terrace-chronological data available for the previous period. Accordingly, the fast incision rates during the last ~140 ka either represent the presence of alternating periods of faster and slower uplift, or accelerated incision due to climate change, and most probably do not record a real acceleration of the long-term uplift. Therefore, we consider the 51 ± 5 m/Ma incision rate, resulting from the trend-line fitted to the dataset between ~3 Ma and ~ 140 ka as a valid approximation of the long-term uplift rate of the Gerecse Hills.

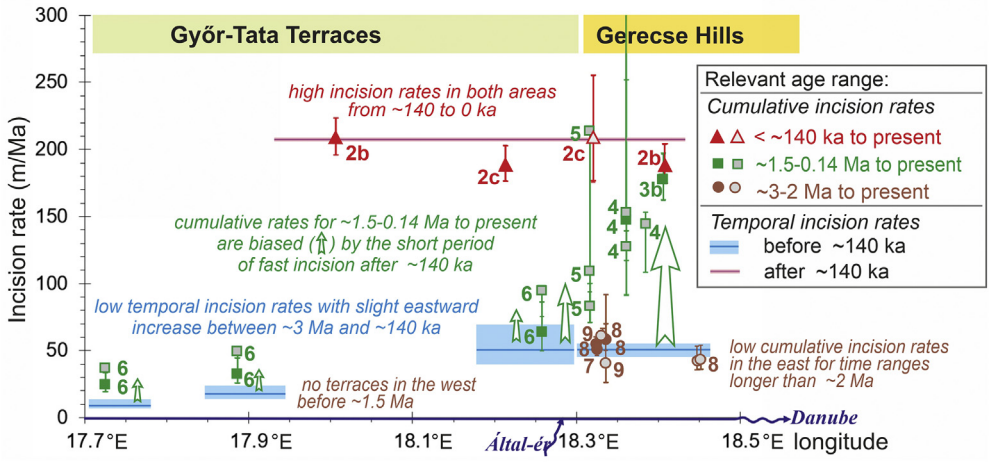

Fig. 9. Spatial and temporal differences of incision rates along the Danube river in the study area from east to west. Note increasing bias of cumulative rates towards faster values with shorter integration times and approaching the GH (indicated by green arrows). For details please refer to the text. Full symbols mean incision/uplift rates calculated from the terrace ages and their uncertainties, open symbols mean maximum incision/uplift rates derived from minimum ages. Numbers indicate the terrace numbers fQ9-2b. Cumulative incision rate data as presented by Tables 1, S1a,b. Temporal incision rates as in section 4.3.1 and Fig. 8, (blue and pink shadows indicate the uncertainties). Dated locations appear on Fig. 2A, B and on Fig. 3A. (For interpretation of the references to colour in this figure legend, the reader is referred to the web version of this article.)

If this fairly constant uplift rate estimated for the last 3 Ma can be extended tentatively until 6 Ma, the sediments of the Lake Pannon must have covered the Gerecse Hills up to 429–460 m a.s.l. This is well in agreement with the ~9 Ma old Upper Miocene sediments described up to 375 m a.s.l. in the Gerecse Hills (Magyar et al., 2017), considering that most probably the Upper Miocene sediments have covered the Gerecse Hills almost entirely in a thickness > 100 m, just the younger part of the succession must have eroded from the higher parts of the range.

5.3. Dependence of cumulative incision rates on the measurement interval

Finnegan et al. (2014) argue that river incision rates into bedrock, determined from dated landforms such as terraces, are influenced by the timescale over which they are measured due to the intermittency of river incision: in general, incision rates increase with decreasing measurement interval. They compiled a global set of incision records and found a negative power-law dependence of incision rate on the considered timescale, up to 10^4–10^7 yrs. Therefore, they suggested a steady-state behaviour of river incision over long measurement intervals. This negative power law dependence of cumulative incision rates of measurement timescale is well observable in our dataset as well (Tables 1, 2, Figs. 7, 9). However, the calculation of temporal incision rates (Fig. 8) suggest the existence of a breakpoint at ~140 ka: until this time the river incision occurred at a fairly constant rate. The faster incision rates are valid only over the last ~140 ka and this period of faster incision rate is responsible for the gradually increasing cumulative incision/uplift rates, as it is demonstrated by Fig. 9).

Accordingly, our findings are in agreement with Finnegan et al. (2014), supporting that increased incision rates over periods of time as short as ~140 ka may bias the cumulative incision rates relevant over 10^6 year timescales. This conclusion is irrespective of the tectonic or climatic forcing of the faster incision rates. Therefore, we emphasize that systematic terrace age determinations on several subsequent terrace horizons are necessary for the calculation of temporal incision rates; as such a dataset enables the distinction between the long-term incision/uplift rates from shorter-term rates biased by temporally faster rates. On the same line of evidences, we suggest that cumulative incision and uplift rates commonly used for the characterisation of spatial and temporal trends of incision and uplift worldwide can be misleading, particularly for time slices only slightly longer than the period of increased incision rate, which divides longer periods of slower uplift, stagnation, bypass or deposition. In order to examine the validity of the above suggestion, rates calculated by this study are compared to published cumulative rates from the neighbouring areas and also from the European continent.

5.4. Comparison of uplift/incision rates to published data

5.4.1. Uplift and incision rates in the TR and its surroundings

On the northern side of the Danube (Hron Upland, Slovakia; Fig. 2B) the number and relative elevation of the terraces, especially that of the higher horizons, is lower compared to the Gerecse Hills. Novel authigenic $^9Be/^{10}Be$ age determination of the locally highest terrace at a relative elevation of ~80 m, suggests that the age of terrace abandonment took place at ~1.4 Ma (Vlačiky et al., 2017, Nová Vieska site, Fig.1A, site 1). The ~57 m/Ma incision rate for the last 1.4 Ma to the north of the Danube is similar to the values calculated for the Gerecse Hills.

In the eastern margin of the TR, U/Th dating of karstwater-related speleothems suggest 150–320 m/Ma incision rate of the Danube during the past 300–200 ka (Leél-Össy et al., 2011; Szanyi et al., 2012, Buda Hills, Fig. 1A, site 2) Before that time, the data suggest a relatively stable karstwater level and moderate uplift rates up to 50 m/Ma.

In the SW part of the TR ^{10}Be exposure age determination of aeolian denudation surfaces indicate an uplift rate of ~50 m/Ma relevant for the last ~1.6 Ma, and ~ 50–80 Ma for the last ~0.9 Ma (Ruszkiczay-Rüdiger et al., 2011, Balaton Highland, Fig. 1A, site 3). In this region basalt volcanism preserved past surface positions and landforms (Martin and Németh, 2004; Csillag, 2004) enabling the estimation of ~50 m/Ma for cumulative surface denudation rate for the last ~3–4 Ma period (Ruszkiczay-Rüdiger et al., 2011).

The reported incision rates are in agreement with the recent, GPS-based, < 350 m/Ma uplift rate at the axis of the TR (Grenerczy et al., 2005; Bus et al., 2009). However, the maximum uplift rate of 1600 m/Ma inferred from ^3He concentrations measured on strath terraces at the Danube Bend (Ruszkiczay-Rüdiger et al., 2005b, Fig. 1A, site 4) appear to be largely overestimated due to insufficient consideration of the effect of surface denudation. The results of the presented study support the conclusions of Ruszkiczay-Rüdiger et al. (2016) suggesting that the previously measured ^3He concentrations of the Danube Bend terraces should rather be interpreted as surface denudation rates and are not suitable for the calculation of the age of terrace abandonment.

We can also extend the comparison to other parts of the Pannonian Basin. On the western margin of the Danube Basin, the minimum luminescence (IRSL) age of > 300 ka of a sand lens within the upper part of the gravel body of a former terrace of the Danube enabled the estimation of a maximum uplift rate of < 87 m/Ma (Zámolyi et al., 2017; (Fig. 1A, site 5, Parndorf Plateau, Nickelsdorf). Šujan et al. (2016) used authigenic $^{10}Be/^9Be$ age determination of terraces on the northern part

of the Danube Basin, suggesting incision rates of ~26 and ~ 4 m/Ma (Veľké Ripňany and Trnava, Fig. 1A, sites 6 and 7, respectively). On the north-western margin of the Danube Basin, Šujan et al. (2017) tentatively calculated a maximum uplift rate of ~26 m/Ma for the last 1.7 Ma based on $^{26}Al/^{10}Be$ burial ages of cave sediments (Malé Karpaty Mts, Fig. 1A, site 8). Neuhuber et al. (2018) used $^{26}Al/^{10}Be$ isochron burial age dating on the sediment infill of a cave, between the Vienna and Danube Basins (Hainburg Hills, Fig. 1A, site 9). Further to the west, the combined CRN and luminescence age determination of Danube terraces in the Vienna Basin suggest differential incision rates of ~81 m/Ma and ~23 m/Ma during the last 340 ka and 250 ka, respectively (Braumann et al., 2019; Schlosshof and Gaenserndorf terraces; Fig. 1A, site 10). They calculated an incision/uplift rate of 36–44 m/Ma for the last ~3.9 Ma. In the Internal Western Carpathians an uplift rate of 30–40 m/Ma was calculated for the last ~3 Ma (Bella et al., 2014) and 20–30 m/Ma relevant for the last 1.6–2.2 Ma (Bella et al., 2019) based on burial age data of cave sediments.

In the Eastern Alps, not far from the western margin of the Danube Basin, Wagner et al. (2010) also dated buried cave sediments and documented an incision rate of ~100 m/Ma over the last 4 Ma (Fig. 1A, site 11). SW from the Pannonian Basin, in Slovenia, the uplift rate quantified by CRN burial age determination was 46–60 m/Ma for the last ~1.86 Ma (Mihevc et al., 2015, Udin Boršt karst, Fig. 1A, site 12) and 200–400 m/Ma in the Snežna jama during the last ~3.5 Ma (Kamnik Alps; Häuselmann et al., 2015; Fig. 1A, site 13).

5.4.2. Incision/uplift rates in a European context

A number of cumulative incision/uplift rates were collected from the European record, in order to reveal whether it is possible to find an inverse relationship between the incision/uplift rates and the time span over which the data were integrated. This overview encompasses cumulative incision/uplift rates from the Pannonian Basin (described in section 5.3) and data reported in different climatic and tectonic regions over Europe. Table 3 shows the referenced uplift /incision rates, which are plotted against the time they are integrated for in Fig. 10.

For timespans integrating over more than ~2.6 Ma most of the incision/uplift rates remain lower than 100 m/Ma. During the Early Pleistocene (~2.6–0.8 Ma) the rates still mostly remain below 100 m/Ma, but with a slightly increasing tendency towards higher values. During the Middle Pleistocene the increasing trend leads to values mostly up to 300 m/Ma. The Late Pleistocene is characterised by higher values, with some exceptionally high estimates up to 2200 m/Ma, but mostly under 600 m/Ma. These tendencies can be observed regardless of the tectonic setting of the studied areas and are similar to those observed in our study area. The faster short-term incision rates, as also recorded in the study area, may be a result of the non-steady-state behaviour of river incision and may not reflect faster uplift over this time (DiBiase, 2014; Finnegan et al., 2014). However, this effect would be similar regardless if the change of incision rate is a true change of uplift rates or just an artefact.

Although the locations of the fastest young incision mostly coincide with tectonically active areas, an overall trend of faster incision/uplift rates over shorter time-spans is valid throughout the dataset irrespective of climatic and tectonic setting of the studied areas, as it was proposed by Finnegan et al. (2014).

Our study is a good example how the apparent acceleration of uplift/incision towards present might be an artefact of a relatively short period of faster incision rate integrated by the longer-term cumulative incision rate data. The uplift/incision rates in the compiled European dataset might also be similarly biased. This effect can only be revealed by a systematic approach in order to obtain a good resolution incision history with temporal incision rates, via age-elevation data pairs for several abandoned river levels.

Table 3
Published incision/uplift rates in Europe in different tectonic settings. For a more detailed description refer to Supplementary section S2 and Table S2.

Cumulative uplift/incision rate (m/Ma)		Reference
Not Alpine	*Alpine*	*setting*
Relevant time range: > 2601 ka to present		
	4	Šujan et al., 2016
	35	Bella et al., 2014
	40	Neuhuber et al., 2018
	50	Ruszkiczay-Rüdiger et al., 2011
	52	Calvet et al., 2015
	53–88	Delmas et al., 2018
90		Malcles et al., 2020
	100	Wagner et al., 2010
	200–400	Häuselmann et al., 2015
250–550		Giachetta et al., 2015
Relevant time range: 2600–801 ka to present		
	26	Šujan et al., 2016
	26	Šujan et al., 2017
	40–60	Mihevc et al., 2015
55–60		Antoine et al., 2007
	57	Vlačiky et al., 2017
	50–80	Ruszkiczay-Rüdiger et al., 2011
33–173	153–160	Schaller et al., 2016
	92	Calvet et al., 2015
70–100		Cunha et al., 2008
	120	Häuselmann et al., 2007
	98–206	Delmas et al., 2018
200		Peters and van Balen, 2007
Relevant time range: 800–201 ka to present		
	23	Braumann et al., 2019
	81	Braumann et al., 2019
10–300		Peters and van Balen, 2007
70–80		Viveen et al., 2012
80–140		Rixhon et al., 2011, 2014
	120	Istrate and Frînculeasa, 2010
	153–159	Schaller et al., 2016
200		Demoulin and Hallot, 2009
	150–320	Szanyi et al., 2012
	230	Temovski et al., 2016
	380–560	Lewis et al., 2017
800		Garcia-Castellanos et al., 2000
	1200	Häuselmann et al., 2007
	1800	Palyvos et al., 2007
Relevant time range: 200–61 ka to present		
	120	Necea et al., 2013
	200–300	Delmas et al., 2018
	300	Istrate and Frînculeasa, 2010
	450	Pennos et al., 2019
	600	Scotti et al., 2014
	800	Brocard et al., 2003
	960	Temovski et al., 2016
Relevant time range: 60 ka to present		
520		Cunha et al., 2008
	400–2200	Necea et al., 2013
	2200	Saillard et al., 2014

5.5. Links between the tectonic forcing factors and the observed vertical deformation pattern

Our study is in agreement with previous inferences highlighting that the several hundred meters uplift of the Transdanubian Range occurred in the absence of measurable crustal thickening (Bada et al., 2007), therefore its origin must be connected to deep lithospheric and asthenospheric processes. Here, we give an overview on the latest model results explaining the origin of the observed tectonic topography of the Pannonian Basin.

Miocene back-arc extension and preceding orogenic evolution of the Pannonian Basin led to one of the hottest and hence, weakest crust and lithosphere in Europe containing rheological heterogeneities (Horváth and Cloetingh, 1996). Such heterogeneities, some of the former syn-rift

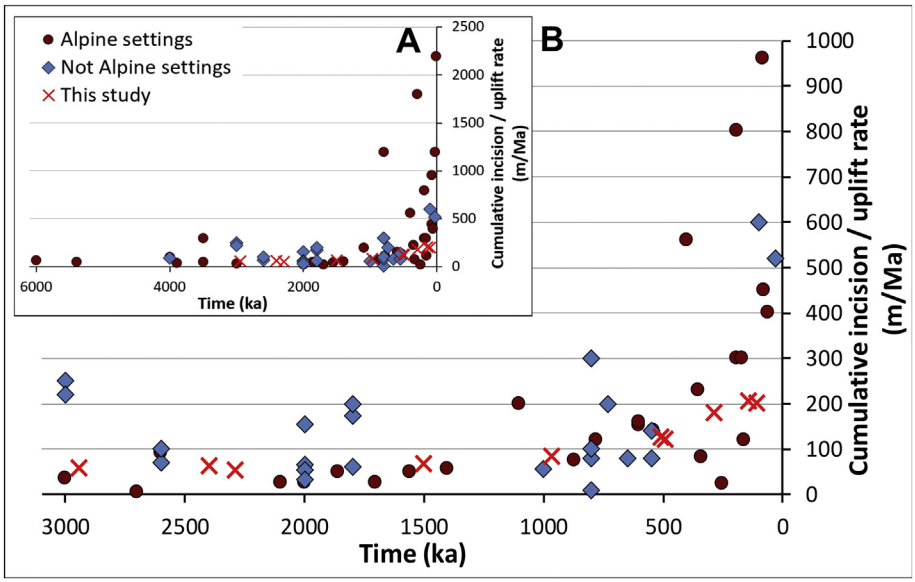

Fig. 10. Cumulative incision/uplift rates throughout Europe plotted against the time over which the rate is integrated. Mean uplift rates and no uncertainties are considered for simplicity. All studies are referred to in Tables 2, 3, S2. and described in sections 5.4.1 and S2. Inset A shows the data between 6 Ma and present, inset B shows the 3 Ma to present timespan in more detail. For colours the reader is referred to the web version of this article.

grabens were inverted and folded in km-scale folds by the slightly radial compression with N–S to NE–SW direction exerted by the push of the Adriatic plate. The weak Pannonian lithosphere was particularly prone to localized deformation even under relatively low differential stresses (Burov and Cloetingh, 1997). Numerical and analogue experiments inferred that far-field stresses lead to a dominant 300–400 km wavelength lithospheric-scale folding of the weak Pannonian lithosphere, where the fold axes are thought to be perpendicular to the direction of compression (Horváth and Cloetingh, 1996; Dombrádi et al., 2010). Interestingly, the SW–NE strike of the uplifting Transdanubian Range is oblique to or parallel with the main compressional direction, and do not satisfy the idea of orthogonality of fold axes and shortening direction. On the other hand, the axis of the uplifting TR is parallel with the main inherited structural trends of the basin (Fig. 11A), such as the Mid-Hungarian Shear zone and similarly striking Cretaceous thrusts (Tari et al., 1999).

3D analogue experiments of Dombrádi et al. (2010) analysed the effect of low strain rate compression on multiple oblique weak zones in the crust representing inherited structures. The modelling explained the observed multi-wavelength folding of the crust as well as the re-activation of strike-slip faults, confirming the crucial role of inherited weak zones. However, field mapping (Fig. 3A) and geophysical imaging (Figs. 6 and 11B) did not confirm high-offset crustal faulting in the northern TR and no such features were reported from other parts of the TR. Few normal faults demonstrated in the northern Danube Basin (Vojtko et al., 2008) are not in line with contraction. The observed deformation pattern (e.g., large-scale tilting and lack of faulting) suggests that Adria-driven shortening and structural inversion alone might not be the main and only driver of the vertical deformation observed in the study area. Similar conclusion was proposed by Legrain et al. (2015) having studied the post-Miocene landscape rejuvenation at the Eastern Alps (Koralpe, Fig. 1A, site 14) They suggested thinning of the mantle part of the lithosphere by slab breakoff or delamination to explain the observed increase in rock uplift.

The above mentioned models aim to explain the first-order neotectonic deformation pattern, but the amplitude of the observed kilometre-scale differential vertical movements has remained enigmatic. A principal limitation of those models was the absence of surface processes, in terms of erosion and sedimentation and the models did not take into account the Late Miocene to recent thermal effects of the lithosphere and asthenosphere. Thermo-mechanically coupled numerical experiments inferred that the initial syn-rift extension could be followed by further asthenosphere dynamics during the classical "post-rift" phase. The development of small-scale convective cells along the previously ascended asthenosphere is superimposed on the overall post-rift cooling in the basin centre. This mechanism leads to differential vertical movements of the surface (Balázs et al., 2017). Additional asthenospheric flow towards the Pannonian Basin has been inferred by seismic shear wave splitting analysis (Kovács et al., 2012; Qorbani et al., 2016,). A systematic NW–SE fast orientation in the entire Eastern European region is interpreted as a result of asthenospheric flow governed by the subduction of the Hellenic slab (e.g., Faccenna et al., 2014). Local upwelling of the asthenosphere is also inferred by volcanological models, and by the study of xenolits below the TR and the margins of the Pannonian Basin (Kovács and Szabó, 2008; Török, 2012; Harangi et al., 2015;). However, solely thermal effects are not enough to create the observed Quaternary subsidence and uplift values in the Danube Basin – TR system.

Modelling the post-rift evolution of the weak Pannonian lithosphere showed that effective lateral heat transport from the elevated asthenosphere beneath the basin induces 30–80 m/Ma uplift rate and erosion near the basin margins (Balázs et al., 2017). These values are on the same order of magnitude as the observed long-term uplift rates in the study area. The modelled vertical tectonic motion is also coupled with the rate of erosion and sedimentation applied in similar models (Burov and Cloetingh, 1997). Similarly, Malcles et al. (2020) quantified the uplift rate for the last ~4 Ma in the southern French Massif Central and concluded that significant part of the calculated ~90 m/Ma uplift was forced by surface processes (erosion and sediment accumulation).

Besides the main driving forces, such as stress transfer by the Adriatic indentation and the inferred asthenospheric flow, the differential vertical motions in the Pannonian Basin are also enhanced by the sediment redistribution from the exposed basement highs towards the local depocenters (Fig. 11). Sediment re-distribution towards the depocenters of the Pannonian Basin led to the deposition of 6–7 km thick Late Miocene to recent sediments including Quaternary succession up to 400–700 m in the Great Hungarian Plain and the Danube- and Drava Basins (Rónai, 1985; Kronome et al., 2012). This basin-scale mass transfer results in elastic flexure of the thermally weakened lithosphere, which enhances differential vertical movements (Balázs et al., 2017). The magnitude of Quaternary surface deformation and sediment redistribution should be compared with the accommodation rate in the Danube and Drava Basins of ~170 m/Ma and ~ 120 m/Ma, respectively (Šujan et al., 2018; Saftič et al., 2003) and the uplift rate of ~30 and ~ 50 m/Ma in the south-eastern and north-western margins of the Danube basin (TR and Malé Karpaty, this study and Šujan et al., 2017,

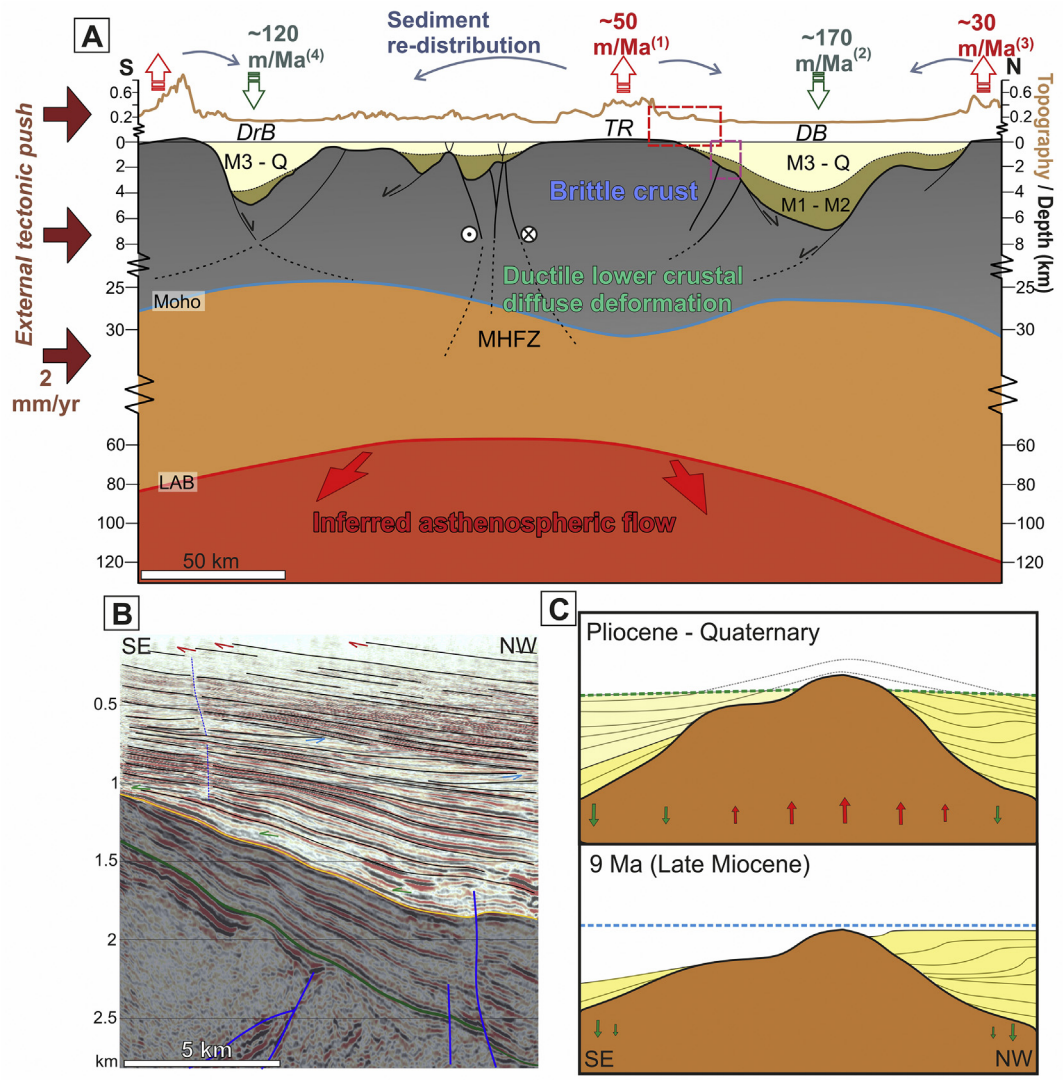

Fig. 11. (A) Simplified lithospheric-scale cross-section over the western part of the Pannonian Basin. For location see Fig. 1A. The study area and the location of the B inset of this figure are indicated by red and purple rectangles, respectively. The section shows the main tectonic and surface processes that control the neotectonic phase of basin evolution. The model takes into account the increased intraplate stress governed by the northward push of the Adriatic microplate and associated induced gravitational stresses (Horváth and Cloetingh, 1996; Bada et al., 2007; Bus et al., 2009; Dombrádi et al., 2010). It also considers the asthenosphere dynamics induced differential vertical movements facilitated by sediment re-distribution and associated lower crustal ductile deformation (Balázs et al., 2017). Crustal thickness is compiled after Horváth et al. (2015), lithosphere-asthenosphere boundary (LAB) is drawn after Tari et al. (1999). DrB – Dráva Basin, TR – Transdanubian Range, DB – Danube Basin. Large arrows in the asthenosphere indicate mantle flow oblique to the section (Qorbani et al., 2016). M1-M2: Lower- to Middle Miocene; M3-Q: Late Miocene to Quaternary. (1) This study, (2) Šujan et al., 2018; (3) Šujan et al., 2017; (4) Saftić et al., 2003. **(B)** Seismic reflection profile showing the dip of the Late Miocene strata towards the Danube Basin, and their truncation towards the TR (for location refer to Figs. 1A, 11A). **(C)** Thematic sketch of the evolution of the TR since the Late Miocene (simplified after Sztanó et al., 2016). Note post-Miocene uplift and denudation of the TR and subsidence of the adjacent basins. (For interpretation of the references to colour in this figure legend, the reader is referred to the web version of this article.)

respectively) (Fig. 11). Furthermore, pressure gradient can develop by erosional unloading of elevated regions and coeval sediment loading in depocenters (Burov and Cloetingh, 1997). This mechanism would induce lower crustal flow from the Danube Basin and Great Hungarian Plain towards the Transdanubian Range, enhancing differential vertical movements (Fig. 11).

Lithospheric flexure and crustal deformation is also linked to climatic variations (Burov and Cloetingh, 1997). A more humid climate facilitates sediment re-distribution and, therefore, enhances elastic flexure and also raises the pressure differences in the lower crust, which finally lead to an increase of the rate of differential vertical movements. Simplified thermo-mechanical models infer that doubling the erosion and sedimentation rate results in additional 200 m of uplift at the exposed margins of the depocenters (Balázs et al., 2017). For an improved understanding of the region's ongoing differential vertical movement patterns it is essential to implement further 3D numerical experiments, which couple all the above mentioned factors into one integrated model.

The studied Danube terraces in the transition between the uplifting TR and the subsiding Danube Basin provide an essential record of the surface expression of the above described tectonic processes, although their amplitudes varied in time and space. An enlargement of the area affected by the uplift could be described sometime between 1.9 Ma and 1.1 Ma, with no considerable change of the uplift rate in the Gerecse Hills. This might be a result of the amplification of deep lithospheric processes coupled with the gradual northward migration of regional neotectonic inversion.

6. Conclusions

The incision rate of the Danube river in the Gerecse Hills, at the margin of the Transdanubian Range, quantified by the compilation of terrace chronological data suggest a steady uplift rate of ~50 m/Ma during Late Pliocene – Quaternary times. The apparent acceleration of river incision during the Late Pleistocene is considered as the result of temporally faster incision outpacing the long-term uplift rate.

The calculation of temporal incision rates revealed that cumulative incision rates are biased towards higher values on a million-year timescale even by a short period (last ~140 ka) of faster incision. This trend of biased rates stemming from integrating short period of fast incision/uplift into the longer term cumulative rates is observable in the European record of cumulative incision/uplift rates as well. Accordingly, these data must be used with caution for the calculation of uplift rates and to derive trends of their change.

Seismic and field data do not indicate large-offset Quaternary brittle structures that could accommodate the observed kilometre-scale differential vertical movements in the vicinity of the Danube Basin. Furthermore, the SW–NE strike of the uplifting Transdanubian Range is oblique to the main compressional direction. We propose that the large wavelength uplift and subsidence anomalies in the area are controlled by the joint effect of crustal and deep Earth processes. Structural inversion governed by the indentation of the Adriatic promontory is complemented by stress variation due to differential sediment loading and further asthenosphere dynamics.

Despite a considerable increase of sediment flux in the sedimentary succession of the northwestern part of the Danube Basin recorded at ~1.2 Ma (Šujan et al., 2018) may correspond to the onset of major Alpine glaciations (mid-Pleistocene climate transition), no simultaneous change in the uplift rate was recorded along the Danube in Hungary. However, the enlargement of the uplifting area from the TR to its north-western margin recorded by the onset of terrace formation in the Győr-Tata Terrace Region (between 1.5 ± 0.4 Ma) might be related to ongoing differential loading of the redistributed sediments and elastic flexure of the weak Pannonian lithosphere.

Funding

This research was supported by several projects funded by the National Research, Development and Innovation Office of Hungary (NKFIH-OTKA, projects 83610, 81530, 113013, 83400, 106197, 124807)and by the Bolyai Postdoctoral Research Programme of the Hungarian Academy of Sciences.

Declaration of Competing Interest

The authors declare that they have no known competing financial interests or personal relationships that could have appeared to influence the work reported in this paper.

Acknowledgements

We dedicate this study to the memory of Frank Horváth, who generously supported this research and improved our knowledge on the formation and evolution of the Pannonian Basin. Gábor Bada is thanked for providing the seismic profiles for this study. AB acknowledges support from the ETH Zürich Postdoctoral Fellowship programme. We are grateful for Peter van der Beek for his comments on a previous version of this manuscript. We are indebted Michal Šujan and Petra Štěpančíková for their reviews helping to improve the manuscript.

Appendix A. Supplementary data

Supplementary data to this article can be found online at https://doi.org/10.1016/j.gloplacha.2020.103263.

References

Antoine, P., Limondin Lozouet, N., Chaussé, C., Lautridou, J.-P., Pastre, J.-F., Auguste, P., Bahain, J.-J., Falguéres, C., Galehb, B., 2007. Pleistocene fluvial terraces from northern France (Seine, Yonne, Somme): synthesis, and new results from interglacial deposits. Quat. Sci. Rev. 26, 2701–2723.

Bada, G., Fodor, L., Székely, B., Timár, G., 1996. Tertiary brittle faulting and stress field evolution in the Gerecse Mountains, northern Hungary. Tectonophys 255, 269–289.

Bada, G., Horváth, F., Dövényi, P., Szafián, P., Windhoffer, G., Cloetingh, S., 2007. Present-day stress field and tectonic inversion in the Pannonian basin. Glob. Planet. Chang. 58, 165–180.

Balázs, A., Burov, E., Matenco, L., Vogt, K., Francois, T., Cloetingh, S., 2017. Symmetry during the syn- and post-rift evolution of extensional back-arc basins: the role of inherited orogenic structures. Earth Planet. Sci. Lett. 462, 86–98.

Balázs, A., Magyar, I., Matenco, L., Sztanó, O., Tőkés, L., Horváth, F., 2018. Morphology of a large paleo-lake: Analysis of compaction in the Miocene–Quaternary Pannonian Basin. Glob. Planet. Chang. 171, 134–147.

Bartha, I.R., Magyar, I., Fodor, L., Csillag, G., Lantos, Z., Tőkés, L., Sztanó, O., 2015. Late Miocene Lacustrine Deltaic Deposit: Integrated Outcrop and Well Data from the Junction of the Danube Basin and Gerecse Hills, Hungary. In: Abstract Book of 31st IAS Meeting of Sedimentology: International Association of Sedimentologists. Polish Geol. Soc. Krakkow, Poland, pp. 54.

Bella, P., Braucher, R., Holec, J., Veselský, M., 2014. Cosmogenic nuclide dating of the burial of allochthonous fluvial sediments in the upper part of the Dobšinská Ice Cave (IVth evolution level of the Stratenská cave system), Slovakia. (in Slovakian with English abstract). Acta Carsologica Slovaca 52 (2), 101–110.

Bella, P., Bosák, P., Braucher, R., Pruner, P., Hercman, H., Minár, J., Veselský, M., Holec, J., Léanni, L., 2019. Multi-level Domica–Baradla cave system (Slovakia, Hungary): Middle Pliocene–Pleistocene evolution and implications for the denudation chronology of the Western Carpathians. Geomorphology 327, 62–79.

Braumann, S.M., Neuhuber, S., Fiebig, M., Schaefer, J.M., Lüthgens, C., 2019. Challenges in constraining ages of fluvial terraces in the Vienna Basin (Austria) using combined isochron burial and pIRIR225 luminescence dating. Quat. Int. 509, 87–102.

Bridgland, D., Westaway, R., 2008. Climatically controlled river terrace staircases: A worldwide Quaternary phenomenon. Geomorph. 98 (3–4), 285–315.

Brocard, G.Y., van der Beek, P.A., Bourlés, D.L., Siame, L.L., Mugnier, J.L., 2003. Long-term fluvial incision rates and postglacial river relaxation time in the French Western Alps from ^{10}Be dating of alluvial terraces with assessment of inheritance, soil development and wind ablation effects. Earth Planet. Sci. Lett. 209, 197–214.

Budai, T., Fodor, L., Zs, Kercsmár, Lantos, Z., Csillag, G., Selmeczi, I., 2018. Geological Map of the Gerecse Mountains 1:50000. Mining and Geological Survey of Hungary, Budapest ISBN 978-963-671-315-7.

Bufe, A., Paola, C., Burbank, D.W., 2016. Fluvial bevelling of topography controlled by lateral channel mobility and uplift rate. Nat. Geosci. 9 (9), 706–710.

Burov, E., Cloetingh, S., 1997. Erosion and rift dynamics: new thermomechanical aspects of post-rift evolution of extensional basins. Earth Planet. Sci. Lett. 150, 7–26.

Bus, Z., Grenerczy, Gy, Tóth, L., Mónus, P., 2009. Active crustal deformation in two seismogenic zones of the Pannonian region — GPS versus seismological observations. Tectonophys. 474, 343–352.

Calvet, M., Gunnell, Y., Braucher, R., Hez, G., Bourles, D., Guillou, V., Delmas, M., Team, Aster, 2015. Cave levels as proxies for measuring post-orogenic uplift: evidence from cosmogenic dating of alluvium-filled-cave in the French Pyrenees. Geomorphology 246, 617–633.

Cantrell, C.A., 2008. Technical note: review of methods for linear least-squares fitting of data and application to atmospheric chemistry problems. Atmos. Chem. Phys. 8, 5477–5487.

Clark, P.U., Archer, D., Pollard, D., Blum, J.D., Rial, J.A., Brovkin, V., Mix, A.C., Pisias, N.G., Roy, M., 2006. The middle Pleistocene transition: characteristics, mechanisms, and implications for long-term changes in atmospheric pCO_2. Quat. Sci. Rev. 25, 3150–3184.

Cloetingh, S., Burov, E., Matenco, L., Beekman, F., Roure, F., Ziegler, P.A., 2013. The Moho in extensional tectonic settings: Insights from thermo-mechanical models. Tectonophys. 609, 558–604.

Cohen, K.M., Gibbard, P., 2016. Global chronostratigraphical correlation table for the last 2.7 million years, v. 2016. Subcommission on Quaternary Stratigraphy, International Commission on Stratigraphy: Cambridge. http://www.quaternary.stratigraphy.org.uk/charts/.

Csillag, G., 2004. Geomorphologic levels of the Kál-Basin and its vicinity. MÁFI Évi Jelentés 2002, 95–110 (in Hungarian with English abstract).

Csillag, G., Fodor, L., Zs, Ruszkiczay-Rüdiger, Lantos, Z., Thamóné, Bozsó E., Babinszki, E., Szappanos, B., Kaiser, M., 2018. Fluvial, fluvial-proluvial, proluvial formations. In: Budai, T. (ed.): Geology of the Gerecse Mountains. Mining and Geological survey of Hungary, Budapest. 131-168, 342–368. ISBN 978-963-671-312-6.

Cunha, P.P., Martins, A.A., Huot, S., Murray, A.S., Raposo, L., 2008. Dating the Tejo river lower terraces in the Ródão area (Portugal) to assess the role of tectonics and uplift. Geomorphology 102, 43–54.

Delmas, M., Calvet, M., Gunnell, Y., Voinchet, P., Manel, C., Braucher, R., Tissoux, H., Bahain, J.-J., Perrenoud, C., Saos, T., 2018. Terrestrial ^{10}Be and electron spin resonance dating of fluvial terraces quantifies quaternary tectonic uplift gradients in the eastern Pyrenees. Quat. Sci. Rev. 193, 188–211.

Demoulin, A., Hallot, E., 2009. Shape and amount of the Quaternary uplift of the western Rhenish shield and the Ardennes (western Europe). Tectonophys. 474, 696–708.

Demoulin, A., Mather, A., Whittaker, A., 2017. Fluvial archives, a valuable record of

vertical crustal deformation. Quat. Sci. Rev. 166, 10–37.
DiBiase, R.A., 2014. River incision revisited. Nature 505, 294–295.
Dombrádi, E., Sokoutis, D., Bada, G., Cloetingh, S., Horváth, H., 2010. Modelling recent deformation of the Pannonian lithosphere: lithospheric folding and tectonic topography. Tectonophys. 484 (1–4), 103–118.
Faccenna, C., Becker, T.W., Auer, L., Billi, A., Boschi, L., Brun, J.P., Capitanio, F.A., Funiciello, F., Horvàth, F., Jolivet, L., 2014. Mantle dynamics in the Mediterranean. Rev. Geophys. 52, 283–332.
Finnegan, N.J., Schumer, R., Finnegan, S., 2014. A signature of transience in bedrock river incision rates over timescales of 10^4–10^7 years. Nature 505, 391–396.
Fodor, L., Csontos, L., Bada, G., Györfi, I., Benkovics, L., 1999. Tertiary tectonic evolution of the Pannonian basin system and neighbouring orogens: a new synthesis of paleostress data. In: Durand, B., Jolivet, L., Horváth, F. & Séranne, M. (eds.) The Mediterranean Basins: Tertiary Extension within the Alpine Orogen. Geol. Soc. London, Spec. Publ. 156. pp. 295–334.
Fodor, L., Bada, G., Csillag, G., Horváth, E., Ruszkiczay-Rüdiger, Zs, Palotás, K., Síkhegyi, F., Timár, G., Cloetingh, S., Horváth, F., 2005. An outline of neotectonic structures and morphotectonics of the western and central Pannonian Basin. Tectonophys. 410 (1–4), 15–41.
Fodor, L., Kercsmár, Zs, Kövér, Sz, 2018. Structure and deformation phases of the Gerecse Hills. In: Budai, T. (ed.): Geology of the Gerecse Mountains. Mining and Geological Survey of Hungary, Budapest. 169-208, 370–386. ISBN 978-963-671-312-6.
Fuchs, M.C., Gloaguen, R., Krbetschek, M., Szulc, M., 2014. Rates of river incision across the main tectonic units of the Pamir identified using optically stimulated luminescence dating of fluvial terraces. Geomorphology 216, 79–92.
Gábris, Gy, Nádor, A., 2007. Long-term fluvial archives in Hungary: response of the Danube and Tisza rivers to tectonic movements and climatic changes during the Quaternary: a review and new synthesis. Quat. Sci. Rev. 26, 2758–2782.
Gábris, Gy, Horváth, E., Novothny, Á., Ruszkiczay-Rüdiger, Zs, 2012. Fluvial and aeolian landscape evolution in Hungary – results of the last 20 years research. Netherl. J. Geosciences 91-1 (2), 111–128.
Garcia-Castellanos, D., Cloetingh, S., Van Balen, R., 2000. Modelling the Middle Pleistocene uplift in the Ardennes–Rhenish Massif: thermo-mechanical weakening under the Eifel? Global and Planet. Change 27, 39–52.
Giachetta, E., Molin, P., Scotti, V.N., Faccena, C., 2015. Plio-Quaternary uplift of the Iberian Chanin (Central-Eastern Spain) from landscape evolution experiments and river profile modeling. Geomorphology 246, 48–67.
Gibbard, P.L., Lewin, J., 2009. River incision and terrace formation in the Late Cenozoic of Europe. Tectonophys. 474, 41–55.
Grenerczy, Gy, Sella, G., Stein, S., Kenyeres, A., 2005. Tectonic implications of the GPS velocity field in the northern Adriatic region. Geophys. Res. Lett. 32, L16311.
Harangi, S., Jankovics, M.É., Sági, T., Kiss, B., Lukas, R., Soós, I., 2015. Origin and geodynamic relationships of the late Miocene to quaternary alkaline basalt volcanism in the Pannonian basin, eastern-central Europe. Int. J. Earth Sci. 104.
Häuselmann, P., Granger, D., Jeannin, P.Y., Lauritzen, S.E., 2007. Abrupt glacial valley incision at 0.8 Ma dated from cave deposits in Switzerland. Geology 35, 143–146.
Häuselmann, P., Mihevc, A., Pruner, P., Horáček, I., Čermák, S., Hercman, H., Sahy, D., Fiebig, M., Zupan Hajna, N., Bosák, P., 2015. Snežna jama (Slovenia): Interdisciplinary dating of cave sediments and implication for landscape evolution. Geomorphology 247, 10–24.
Hók, J., Kysel, R., Kováč, M., Moczo, P., Kristek, J., Kristeková, M., Šujan, M., 2016. A seismic source zone model for the seismic hazard assessment of Slovakia. Geol. Carpath. 67 (3), 273–288.
Horváth, F., Cloetingh, S., 1996. Stress-induced late-stage subsidence anomalies in the Pannonian basin. Tectonophys. 266, 287–300.
Horváth, F., Musitz, B., Balázs, A., Végh, A., Uhrin, A., Nádor, A., Koroknai, B., Pap, N., Tóth, T., Wórum, G., 2015. Evolution of the Pannonian basin and its geothermal resources. Geothermics 53, 328–352.
Istrate, A., Frînculeasa, M., 2010. Paleoclimatic conditions of evolution in the final stage of relief construction in Mostiştea plain. The Annals of Valahia Univ. of Târgovişte. Geographical Series 10, 13–26.
Kele, S., 2009. Study of Freshwater Limestones from the Carpathian Basin: paleoclimatological and Sedimentological Implications. PhD Thesis. Eötvös Loránd University, Hungary. pp. 176.
Kovács, I., Szabó, C., 2008. Middle Miocene volcanism in the vicinity of the middle Hungarian zone: evidence for an inherited enriched mantle source. J. Geodyn. 45 (1), 1–17.
Kovács, I., Falus, Gy, Stuart, G., Hidas, K., Szabó, C.S., Flower, M.F.J., Hegedűs, E., Posgay, K., Zilahi-Sebess, L., 2012. Seismic anisotropy and deformation patterns in upper mantle xenoliths from the central Carpathian–Pannonian region: Asthenospheric flow as a driving force for Cenozoic extension and extrusion? Tectonophys. 514–517, 168–179.
Kronome, B., Fordinál, K., Baráth, I., Maglay, J., Nagy, A., Uhrin, A., 2012. Base Quaternary model horizon depth - pilot area Danube Basin. In: Maros, G. (Ed.), Summary Report of Geological Models. TransEnergy – Transboundary Geothermal Energy Resources of Slovenia, Austria, Hungary and Slovakia, pp. 133–140.
Leél-Össy, Sz, Szanyi, Gy, Surányi, G., 2011. Minerals and speleothems of the József-hegy Cave (Budapest, Hungary). Int. J. Speleol. 40, 191–203.
Legrain, N., Dixon, J., Stüwe, K., von Blanckenburg, F., Kubik, P., 2015. Post-Miocene landscape rejuvenation at the eastern end of the Alps. Lithosphere 7 (1), 3–13.
Lewis, C.J., Sancho, C., McDonald, E.V., Peña-Monné, J.L., Pueyo, E.L., Rhodes, E., Valle, M., Soto, R., 2017. Post-tectonic landscape evolution in NE Iberia using staircase terraces: combined effects of uplift and climate. Geomorphology 292, 85–103.
Lisiecki, L.E., Raymo, M.E., 2005. A Pliocene-Pleistocene stack of 57 globally distributed benthic $\delta^{18}O$ records. Paleoceanography 20, PA1003.
Lithgow-Bertelloni, C., Silver, P.G., 1998. Dynamic topography, plate driving forces and the African superswell. Nature 395, 269–272.
Madarás, J., Fojtíková, L., Hrašna, M., Petro, Ľ., Ferianc, D., Briestensky, M., 2012. Definition of the seismic active regions in Slovakia based on historical earthquake records and current monitoring of tectonic and seismic activity. Mineralia Slovaca 44, 351–364 ISSN 0369-2086 (in Slovakian, with English summary).
Maddy, D., Bridgland, D.R., Westaway, R., 2001. Uplift-driven valley incision and climate-controlled river terrace development in the Thames Valley, UK. Quat. Int. 79, 23–36.
Magyar, I., Radivojević, D., Sztanó, O., Synak, R., Ujszászi, K., Pócsik, M., 2013. Progradation of the paleo-Danube shelf margin across the Pannonian Basin during the Late Miocene and Early Pliocene. Glob. Planet. Chang. 103, 168–173.
Magyar, I., Sztanó, O., Csillag, G., Kercsmár, Zs., Katone, L., Lantos, Z., Bartha, I.R., Fodor, L. 2017. Pannonian molluscs and their localities in the Gerecse Hills, Transdanubian Range: stratigraphy, palaeoenvironment, geological evolution (in Hungarian with English summary). Földt. Közl. 147/2, 149–176.
Malcles, O., Vernant, P., Chéry, J., Camps, P., Cazes, G., Ritz, J.F., Fink, D., 2020. Determining the Plio-Quaternary uplift of the southern French Massif Central; a new insight for intraplate orogen dynamics. Solid Earth 11 (1), 241–258.
Martin, U., Németh, K., 2004. Mio/Pliocene phreatomagmatic volcanism in the Western Pannonian Basin. Geol. Hungarica. Ser. Geol. 26, 1–192.
Maţenco, L., Munteanu, I., ter Borgh, M., Stanica, A., Tilita, M., Lericolais, G., Dinu, C., Oaie, G., 2016. The interplay between tectonics, sediment dynamics and gateways evolution in the Danube system from the Pannonian Basin to the western Black Sea. Sci. Total Environ. 543, 807–827.
Maţenco, L., Radivojević, D., 2012. On the formation and evolution of the Pannonian Basin: constraints derived from the structure of the junction area between the Carpathians and Dinarides. Tectonics 31 (6), TC6007.
Mihevc, A., Bavec, M., Häuselmann, P., Fiebig, M., 2015. Dating of the Udin Boršt conglomerate terrace and implication for tectonic uplift in the northern part of the Ljubljana Basin (Slovenia). Acta Carsologica 44 (2), 169–176.
Necea, D., Fielitz, W., Kadereit, A., Andriessen, P.A.M., Dinu, C., 2013. Middle Pleistocene to Holocene fluvial terrace development and uplift-driven valley incision in the SE Carpathians. Romania. Tectonophys. 602, 332–354.
Neuhuber, S., Plan, L., Gier, S., Bodelenz, F., Fiebig, M., 2018. Burial dating of cave sediments reveal uplift/incision at the Carpathian-Alpine border (Hainburg Hills). Geologica Balcanica, XXI International Congress of the CBGA, Salzburg, Austria, September 10–13, 2018, Abstracts, p. 264.
Olszak, J., 2017. Climatically controlled terrace staircases in uplifting mountainous areas. Glob. Planet. Chang. 156, 13–23.
Palyvos, N., Sorel, D., Lemeille, F., Mancini, M., Pantosti, D., Julia, R., Triantaphyllou, M., De Martini, P.M., 2007. Review and new data on uplift rates at the W termination of the Corinth Rift and the NE Rion graben area (Achaia, NW Peloponnesos). Bull. Geol. Soc. Greece 40 (1), 412–424.
Pécsi, M., 1959. Formation and Geomorphology of the Danube Valley in Hungary (in Hungarian with German Summary). Akadémiai Kiadó, Budapest 346 p.
Pécsi, M., Scheuer, Gy, Schweitzer, F., 1982. Geomorphological position and chronological classification of Hungarian travertines. Quat. Stud. in Hungary 117–133 Budapest.
Pennos, C., Lauritzen, S.E., Vouvalidis, K., Cowie, P., Pechlivanidou, S., Gkarlaouni, C., Styllas, M., Tsourlos, P., Mouratidis, A., 2019. From subsurface to surface: a multidisciplinary approach to decoding uplift histories in tectonically-active karst landscapes. Earth Surf. Process. Landf. 44, 1710–1721.
Peters, G., van Balen, R., 2007. Pleistocene tectonics inferred from fluvial terraces of the northern Upper Rhine Graben. Germany. Tectonophys. 430, 41–65.
Qorbani, E., Bokelmann, G., Kovács, I., Horváth, F., Falus, G., 2016. Deformation in the asthenospheric mantle beneath the Carpathian-Pannonian Region. J. Geophys. Res. Solid Earth 121, 6644–6657.
Ratschbacher, L., Frisch, W., Linzer, H.G., Merle, O., 1991. Lateral extrusion in the Eastern Alps, part 2: Structural analysis. Tectonics 10, 257–271.
Reimer, P.J., Bard, E., Bayliss, A., Beck, J.W., Blackwell, P.G., Bronk Ramsey, C., Grootes, P.M., Guilderson, T.P., Haflidason, H., Hajdas, I., Hatte, C., Heaton, T.J., Hoffmann, D.L., Hogg, A.G., Hughen, K.A., Kaiser, K.F., Kromer, B., Manning, S.W., Niu, M., Reimer, R.W., Richards, D.A., Scott, E.M., Southon, J.R., Staff, R.A., Turney, C.S.M., van der Plicht, J., 2013. IntCal13 and Marine13 radiocarbon age calibration curves 0-50,000 years cal BP. Radiocarbon 55 (4), 1869–1887.
Rixhon, G., Braucher, R., Bourlès, D., Siame, L., Bovy, B., Demoulin, A., 2011. Quaternary river incision in NE Ardennes (Belgium) – Insights from $^{10}Be/^{26}Al$ dating of river terraces. Quat. Geochronol. 6, 273–284.
Rixhon, G., Bourlès, D., Braucher, R., Siame, L., Cordy, J.-M., Demoulin, A., 2014. ^{10}Be dating of the Main Terrace level in the Ambléve valley (Ardennes, Belgium): new age constraint on the archaeological and palaeontological filling of the Belle-Roche palaeokarst. Boreas 43 (2), 528–542.
Rónai, A., 1985. Quaternary Geology of the Great Hungarian Plain (in Hungarian). Geol. Hungarica, Ser. Geol. 21. (446 p).
Ruszkiczay-Rüdiger, Zs, Fodor, L., Bada, G., Leél-Össy, Sz, Horváth, E., Dunai, T.J., 2005a. Quantification of Quaternary vertical movements in the central Pannonian Basin: A review of chronologic data along the Danube River. Hungary. Tectonophys. 410 (1–4), 157–172.
Ruszkiczay-Rüdiger, Zs, Dunai, T.J., Bada, G., Fodor, L., Horváth, E., 2005b. Middle to Late Pleistocene uplift rate of the Hungarian Mountain Range at the Danube Bend (Pannonian Basin) using in situ produced ^{3}He. Tectonophys. 410 (1–4), 173–187.
Ruszkiczay-Rüdiger, Zs, Fodor, L., Horváth, E., 2007. Neotectonics and Quaternary landscape evolution of the Gödöllő Hills, Central Pannonian Basin. Hungary. Glob. Planet. Change 58, 181–196.
Ruszkiczay-Rüdiger, Zs, Braucher, R., Csillag, G., Fodor, L., Dunai, T.J., Bada, G., Bourlés, D., Müller, P., 2011. Dating Pleistocene aeolian landforms in Hungary, Central

Europe, using in situ produced cosmogenic ^{10}Be. Quat. Geochronol. 6, 515–529.
Ruszkiczay-Rüdiger, Zs, Braucher, R., Novothny, Á., Csillag, G., Fodor, L., Molnár, G., Madarász, B., Team, ASTER, 2016. Tectonic and climatic forcing on terrace formation: Coupling in situ produced ^{10}Be depth profiles and luminescence approach, Danube River, Hungary, Central Europe. Quat. Sci. Rev. 131, 127–147.
Ruszkiczay-Rüdiger, Zs, Csillag, G., Fodor, L., Braucher, R., Novothny, Á., Thamó-Bozsó, E., Virág, A., Pazonyi, P., Timár, G., Team, ASTER, 2018. Integration of new and revised chronological data to constrain the terrace evolution of the Danube River (Gerecse Hills, Pannonian Basin). Quat. Geochronol. 48, 148–170.
Sacchi, M., Horváth, F., Magyari, O., 1999. Role of unconformity-bounded units in the stratigraphy of the continental record: a case study from the Late Miocene of westen Pannonian Basin, Hungary. – In: Durand, B., Jolivet, L., Horváth, F., Séranne, M. (Eds.), The Mediterranean Basins: Tertiary extension within the Alpine Orogen. - Geological Society Special Publications 156. pp. 357–390.
Saftič, B., Velic, J., Sztanó, O., Juhász, Gy, Ivkovic, Z., 2003. Tertiary subsurface facies, source rocks and hydrocarbon reservoirs in the SW part of the Pannonian Basin (Northern Croatia and South-Western Hungary). Geol. Croatica 56, 101–122.
Saillard, M., Petit, C., Rolland, Y., Braucher, R., Bourlès, D.L., Zerathe, S., Revel, M., Jourdon, A., 2014. Late Quaternary incision rates in the Vésubie catchment area (Southern French Alps) from in situ-produced ^{36}Cl cosmogenic nuclide dating: Tectonic and climatic implications. J. Geophys. Res. Earth Surf. 119. https://doi.org/10.1002/2013JF002985.
Schaller, M., Ehlers, T.A., Stor, T., Torrent, J., Lobato, L., Christl, M., Vockenhuber, C., 2016. Timing of European fluvial terrace formation and incision rates constrained by cosmogenic nuclide dating. Earth Planet. Sci. Lett. 451, 221–231.
Scheuer, Gy, Schweitzer, F., 1988. Freshwater limestones of the Gerecse and Buda Hills (in Hungarian). Földr. Tanulm. 20. Akad. Kiadó, Budapest, pp. 129.
Scotti, V.N., Molin, P., Faccenna, C., Soligo, M., Casas-Sainz, A., 2014. The influence of surface and tectonic processes on landscape evolution of the Iberian Chain (Spain): quantitative geomorphological analysis and geochronology. Geomorphology 206, 37–57.
Sierralta, M., Kele, S., Melcher, F., Hambach, U., Reinders, J., Van Geldern, R., Frechen, M., 2010. Uranium-sereies dataing of travertine from Süttő: implications for reconstruction of environmental change in Hungary. Quat. Int. 222, 178–193.
Sipos-Benkő, K., Márton, E., Fodor, L.I., Pethe, M., 2014. An integrated magnetic susceptibility anisotropy (AMS) and structural geological study on Cenozoic clay rich sediments from the Transdanubian Range. Central Eur. Geology 51 (1), 21–52.
Starkel, L., 2003. Climatically controlled terraces in uplifting mountain areas. Quat. Sci. Rev. 22, 2189–2198.
Štor, T., Schaller, M., Merchel, S., Martínek, K., Rittenour, T., Rugel, G., Scharf, A., 2019. Quaternary evolution of the Ploučnice River system (Bohemian Massif) based on fluvial deposits dated with optically stimulated luminescence and in situ produced cosmogenic nuclides. Geomorphology 329, 152–169.
Šujan, M., Rybár, S., 2014. The development of Pleistocene river terraces in the eastern part of the Danube Basin (in Slovakian with English abstract). Acta Geol. Slovaca 6 (2), 107–122.
Šujan, M., Braucher, R., Kováč, M., Bourlès, D.L., Rybár, S., Guillou, V., Hudáčková, N., 2016. Application of the authigenic ^{10}Be/^{9}Be dating method to Late Miocene–Pliocene sequences in the northern Danube Basin (Pannonian Basin System): confirmation of heterochronous evolution of sedimentary environments. Glob. Planet. Chang. 137, 35–53.
Šujan, M., Lačný, A., Braucher, R., Magdolen, P., Team, ASTER, 2017. Early Pleistocene age of fluvial sediment in the Stará Garda Cave revealed by ^{26}Al/^{10}Be burial dating: implications for geomorphic evolution of the Malé Karpaty Mts. (Western Carpathians). Acta Carsologica 46 (2), 251–264.
Šujan, M., Braucher, R., Rybár, S., Maglay, J., Nagy, A., Fordinál, K., Šarinová, K., Sýkora, M., Józya, S., Kovač, M., Team, ASTER, 2018. Revealing the late Pliocene to Middle Pleistocene alluvial archive in the confluence of the Western Carpathian and Eastern Alpine rivers: ^{26}Al/^{10}Be burial dating from the Danube Basin (Slovakia). Sediment. Geol. 377, 131–146.
Šujan, M., Braucher, R., Tibenský, M., Fordinál, K., Rybár, S., Kováč, M., 2020. Effects of spatially variable accommodation rate on channel belt distribution in an alluvial sequence: Authigenic ^{10}Be/^{9}Be-based Bayesian age-depth models applied to the upper Miocene Volkovce Fm. (northern Pannonian Basin System, Slovakia). Sediment. Geol. 397 105566.
Szanyi, Gy, Surányi, G., Leél-Össy, Sz, 2012. Cave development and Quaternary uplift history in the Central Pannonian Basin derived from speleothem ages. Quat. Geochronol. 14, 18–25.
Sztanó, O., Kováč, M., Magyar, I., Šujan, M., Fodor, L., Uhrin, A., Rybár, S., Csillag, G., Tőkés, L., 2016. Late Miocene lithostratigraphy of the Danube / Kisalföld Basin: interregional correlation of depositional systems, stratigraphy and structural evolution. Geol. Carpath. 67, 525–542.
Sztanó O.; Budai S.; Magyar I.; Fodor L.; Csillag G.; Nadrai J., Lessons from a coarse-grained lacustrine paleo-tsunamite: an integrated study of a late Miocene boulderly cobble gravel. Global and Planetary Change. (submitted).
Tari, G., 1994. Alpine tectonics of the Pannonian Basin. PhD. Thesis, Rice University, Houston. pp. 1–501.
Tari, G., Dövenyi, P., Dunkl, I., Horvath, F., Lenkey, L., Ştefănescu, M., Szafián, P., Tóth, T., 1999. Lithospheric structure of the Pannonian basin derived from seismic, gravity and geothermal data, in The Mediterranean Basins: Extension Within the Alpine Orogen, Geol. Soc. Spec. Publ., 156, In. Durand, B. et al. (ed) 215–250.
Temovski, M., Pruner, P., Hercman, H., Bosák, P., 2016. Cave response to environmental changes in Late Pleistocene: study of Budimirica Cave sediments. Macedonia. Geol. Croatica 69 (3), 307–316.
Tomljenović, B., Csontos, L., 2001. Neogene-Quaternary structures in the border zone between Alps, Dinarides and Pannonian Basin (Hrvatsko zagorje and Karlovac Basins, Croatia). Int. J. Earth Sci. 90 (3), 560–578.
Török, K., 2012. On the origin and fluid content of some rare crustal xenoliths and their bearing on the structure and evolution of the crust beneath the Bakony–Balaton Highland Volcanic Field (W-Hungary). Int. J. Earth Sci. DOI. https://doi.org/10.1007/s00531-011-0743-2.
Török, Á., Mindszenty, A., Claes, H., Kele, S., Fodor, L., Swennen, R., 2017. Geobody architecture of continental carbonates: “Gazda” travertine quarry (Süttő, Gerecse Hills, Hungary). Quat. Int. 437, 164–185.
Török, Á., Claes, H., Brogi, A., Liotta, D., Tóth, Á., Mindszenty, A., Kudó, I., Kele, S., Huntington, K.W., Shen, C.-C., Swennen, R., 2019. A multi–methodological approach to reconstruct the configuration of a travertine fissure ridge system: The case of the Cukor quarry (Süttő, Gerecse Hills, Hungary). Geomorphology 345, 106836.
Tóth, L., Mónus, P., Kiszely, M., 2002. Seismicity in the Pannonian Region - earthquake facts. In: Cloetingh, S., Horváth, F., Bada, G., Lankreijer, A. (Eds.), Neotectonics and Surface Processes: The Pannonian Basin and Alpine/Carpathian System. EGU St. Mueller Spec. Publ. Ser, vol. 3. pp. 9–28.
Ujházy, K., Gábris, Gy, Frechen, M., 2003. Ages of periods of sand movement in Hungary determined through luminescence measurements. Quat. Int. 111, 91–100.
Ustaszewski, K., Herak, M., Tomljenović, B., Herak, D., Matej, S., 2014. Neotectonics of the Dinarides-Pannonian Basin transition and possible earthquake sources in the Banja Luka epicentral area. J. Geodyn. 82, 52–68.
Vandenberghe, J., 2015. River terraces as a response to climatic forcing: formation processes, sedimentary characteristics and sites for human occupation. Quat. Int. 370, 3–11.
Viveen, W., Braucher, R., Bourlés, D., Schoorl, J.M., Veldkamp, A., van Balen, R.T., Wallinga, Fernandez-Mosquera, Vidal-Romani, J.R., Sanjurjo-Sanchez, J., 2012. A 0.65 Ma chronology and incision rate assessment of the NW Iberian Miño River terraces based on ^{10}Be and luminescence dating. Glob. Planet. Change 94-95, 82–100.
Vlačiky, M., Šujan, M., Rybár, S., Braucher, R., 2017. Nová Vieska locality: fauna, sediments and their dating - new results. In: Šimon, L., Ozdínová, S., Kováčiková, M., (Eds.) 15th Christmas Geological Workshop SGS - New Findings of the Structure and Evolution of the Western Carpathians. Mente et Malleo (MeM) - Newsletter of the Slovak Geol. Soc. (SGS) 2, 57 (in Slovakian).
Vojtko, R., Hók, J., Kováč, M., Sliva, L., Joniak, P., Šujan, M., 2008. Pliocene to Quaternary stress field change in the western part of the Central Western Carpathians (Slovakia). Geol. Quart. 52 (1), 19–30.
Vrabec, M., Fodor, L., 2006. Late Cenozoic tectonics of Slovenia: Structural styles at the northeastern corner of the Adriatic microplate. In: Pinter, N., Grenerczy, Gy., Weber, J., Stein, S., Medak, D. (eds): The Adria microplate: GPS Geodesy, Tectonics, and Hazards. NATO Science Series IV, 61, 151–168, Springer.
Vrabec, M., Pavlovčič Prešeren, P., Stopar, B., 2006. GPS study (1996–2002) of active deformation along the Periadriatic fault system in northeastern Slovenia: tectonic model. Geol. Carpath. 57 (1), 57–65.
Wagner, T., Fabel, D., Fiebig, M., Häuselmann, P., Sahy, D., Xu, S., Stüwe, K., 2010. Young uplift in the non-glaciated parts of the Eastern Alps. Earth Planet. Sci. Lett. 295, 159–169.
Wéber, Z., 2016. Probabilistic waveform inversion for 22 earthquake moment tensors in Hungary: new constraints on the tectonic stress pattern inside the Pannonian basin. Geophys. J. Int. 204, 236–249.
Wéber, Z., Süle, B., 2014. Source Properties of the 29 January 2011 ML 4.5 Oroszlány (Hungary) Mainshock and Its Aftershocks. Bull. Seismol. Soc. Am. 104 (1), 113–127.
Zámolyi, A., Salcher, B., Draganits, E., Exner, U., Wagreich, M., Gier, S., Fiebig, M., Lomax, J., Surányi, G., Diel, M., Zámolyi, F., 2017. Latest Pannonian and Quaternary evolution at the transition between Eastern Alps and Pannonian Basin: new insights from geophysical, sedimentological and geochronological data. Int. J. Earth Sci. 106 (5), 1695–1721.